

Developing Advanced Catalysts for the Conversion of Polyolefinic Waste Plastics into Fuels and Chemicals

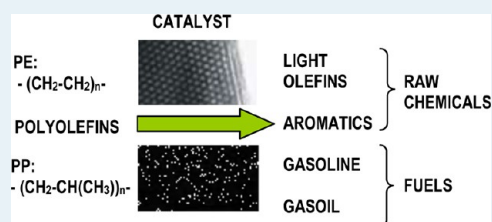
D. P. Serrano,^{*,†,§} J. Aguado,[‡] and J. M. Escola[‡]

[†]Department of Chemical and Energy Technology and [‡]Department of Chemical and Environmental Technology, ESCET Rey Juan Carlos University, c/Tulipán s/n, 28933, Móstoles, Madrid, Spain

[§]IMDEA Energy Institute, Avenida Ramón de la Sagra, 3, 28935, Móstoles, Madrid, Spain

ABSTRACT: The present review is aimed at exploring the field of the catalytic cracking of polyolefins over solid acids, focusing on the role played by the catalysts toward the synthesis of fuels and chemicals as well as on the reaction systems currently used. Initially, conventional solid acids, such as micrometer sized crystal zeolites and silica–alumina, were used to establish the relationship among their activity, selectivity, and deactivation in the polyolefin cracking and the inherent properties of the catalysts (acidity, pore structure); however, the occurrence of steric and diffusional hindrances for entering the zeolite micropores posed by the bulky nature of the polyolefins highlighted the importance of having easily accessible acid sites, either through mesopores or by a high external surface area. This fact led toward the investigation of mesoporous materials (Al-MCM-41, Al-SBA-15) and nanozeolites, which allowed increasing the catalytic activities, especially for the case of polypropylene. Further advances have come by the application of hierarchical zeolites whose bimodal micropore–mesopore size distribution has turned them into the most active catalysts for polymer cracking. In this regard, hierarchical zeolites may be regarded as a clear breakthrough, and it is expected that future research on them will bring new achievements in the field of catalytic cracking of polyolefins. In addition, other materials with high accessibility toward the active sites, such as extra-large pore zeolites, delaminated zeolites, or pillared zeolite nanosheets, can also be considered potentially promising catalysts. From a commercial point of view, two-step processes seem to be the most feasible option, including a combination of thermal treatments with subsequent catalytic conversion and reforming, which allows the catalytic activity to be preserved against different types of deactivation.

KEYWORDS: polyolefin, cracking, zeolites, MCM-41, hierarchical zeolites



1. INTRODUCTION

Polyolefins are commodity materials of utmost importance since they constitute the group of plastics with the highest world consumption. In Europe, the demand of plastics in 2010 was around 46.4 million tons, wherein polyolefins accounted for 48% of the total.¹ Polyolefin plastics are mostly low density polyethylene (LDPE), linear low density polyethylene (LLDPE), high density polyethylene (HDPE), and polypropylene (PP) and find use in many common applications, such as pipes, films, packaging, insulation, etc. However, after finishing their lifetime (which is usually short, less than 1 year), they end up as a waste. According to Plastics Europe,¹ the amount of plastic wastes obtained in 2010 was 24.7 million tons, polyolefins being their main components.

Since the mid 90s, the EU has been aware of the magnitude of the problem and has set up several directives promoting more stringent recycling and recovery rates to reduce the extent of landfilling.² Until now, these directives have proven relatively successful since landfilling of plastics has decreased to 42% in the whole EU, and in some countries, such as Switzerland, Germany or Austria, <5% of the plastic wastes are disposed of in landfills.

The most usual ways of dealing with these wastes are mechanical recycling and incineration with energy recovery.

Mechanical recycling, which turns the plastic waste into another plastic for similar or slightly inferior applications by melting and subsequent remolding, is particularly suitable for polyolefins, since they are thermoplastics. However, this treatment has shown several important limitations, such as the progressive loss of quality of the polyolefins after successive cycles of melting–remolding and the need of segregating the polyolefins³ or using compatibilizers⁴ with polyolefin mixtures to attain adequate mechanical resistance. Therefore, it seems that mechanical recycling of polyolefins is not a definitive treatment, and sooner or later it will require other treatments to eliminate the waste. The most usual alternative in many countries for the treatment of waste plastics is incineration with energy recovery, taking advantage of the high calorific power of the polyolefins (~40–44 MJ/kg), similar to petroleum (42 MJ/kg), since modern incinerators can retrieve up to 60% of this energy.⁵ However, this option is often socially rejected because of the risk of emission of toxic compounds, such as dioxins and furans.

Consequently, the current situation might be described as a search of mature technologies that can eliminate and process

Received: May 31, 2012

Revised: July 27, 2012

Published: July 30, 2012

these polyolefin wastes with the lowest environmental impact and the highest possible profitability. Gasification of plastic wastes to yield synthesis gas has been proposed as one of these technologies, but it is very costly and requires the construction of large plants to be profitable.^{6,7} In this regard, catalytic cracking technologies toward transportation fuels (gasoline, diesel) and chemicals are more flexible and are receiving increased attention, since in a context of growing prices of crude oil, its profitability improves considerably.

Three ways may be envisaged for carrying out the catalytic pyrolysis of the plastic wastes. The first option consists of performing the catalytic cracking by contacting directly the catalyst with the plastic waste feed. In this case, the bulky nature of the plastic macromolecule and its inherent huge viscosity causes the appearance of both mass and heat transfer constraints. In addition, the presence of different impurities contained in the plastic wastes feed, which can work as potential poisons, may provoke the catalyst deactivation. The second option, which can solve these problems, is to perform initially a thermal cracking step of the plastic wastes, followed by a catalytic reforming of the heavy oil obtained previously. Thus, the viscosity of the feed decreases and the impurities may be removed by different treatments, avoiding direct contact with the catalyst. A third choice consists of performing a thermal cracking of the plastic wastes feed, followed by a catalytic hydroreforming with a view to optimizing further the properties of the obtained final hydrocarbon mixture.

This review is aimed at providing insight into the field of catalytic cracking of polyolefins, highlighting the key role played by the catalyst not only for enhancing the activity of the cracking but also for the preparation of hydrocarbon mixtures with enhanced fuel properties. This work updates a previous one by the present authors² and is more specific, since it is mainly focused on the catalyst properties, discussing thoroughly the aspects that determine the catalytic performance (activity, selectivity, deactivation, and kinetics) and highlighting the future trends in the field.

2. CATALYTIC CRACKING VERSUS THERMAL CRACKING

The catalytic cracking of polyolefins at 400–550 °C gives rise to hydrocarbon mixtures completely different from those achieved after pure thermal cracking in the absence of a catalyst. This fact is due in part to the different nature of their respective cracking mechanisms. Thermal cracking takes place by means of a radical chain transfer mechanism, comprising the usual initiation, propagation, and termination steps. Accordingly, the polymer backbone is broken off into a diversity of fragments by the homolytic cleavage of the carbon–carbon bond, leading finally to the formation of a broad hydrocarbon distribution wherein their main components in each fraction are the *n*-paraffin, the 1-alkene, and the corresponding alkadiene.⁸ No rearrangement of the radicals occurs during the thermal cracking, so the only branched products obtained are formed via reaction between two radicals. Hence, in the thermal cracking of HDPE, a broad hydrocarbon mixture is obtained, comprising C₁–C₆₀ hydrocarbons.⁹ As the temperature increases, the share of low-molecular-weight products is enhanced.¹⁰ In addition, the proportion of aromatics obtained at 400–500 °C is rather low, although it is augmented on increasing the temperature and, in addition, when the pyrolysis gas is subsequently recirculated and used as fluidizing gas. In this way, Kaminsky et al.¹¹ reported benzene contents of 19.2%

in the oils attained from the pyrolysis of polyethylene at 740 °C in a fluidized bed reactor. On the other hand, Kaminsky also proved that by using steam as a fluidizing agent and temperature above 700 °C, high yields of ethene and propene (15–30%) might be achieved.¹² Unlike in the case of the pyrolysis of other plastics (e.g., polymethylmethacrylate), thermal cracking of polyolefins does not allow recovery of the constituting monomer in reasonable amounts. Therefore, thermal cracking of the polyolefins yields only mixtures of hydrocarbons, which may be useful as low-quality fuels, for the production of waxes, or (if steam cracking is used) for the manufacture of light olefins.

Catalytic cracking of polyolefins shows several advantages with regard to the previously commented thermal pyrolysis. First, catalytic cracking proceeds through a carbocationic mechanism, wherein the carbocation is formed by abstraction of a hydride ion by a Lewis acid site to form carbenium ions or by protonation of the hydrocarbon on Brønsted acid sites, generating carbonium ions.¹³ Once these carbocations are formed, different acid-catalyzed reactions may occur over the acid sites, such as isomerization, oligomerization cyclization, aromatization, and cracking. Cyclization and aromatization proceed by means of hydrogen transfer reactions, whereas cracking usually takes place by means of β-scission reactions. These cracking reactions may occur at random in the polymer backbone or preferentially at the end of the chain. The occurrence of one or other possibility depends chiefly on the acidity and pore structure of the chosen catalyst.¹⁴ Figure 1

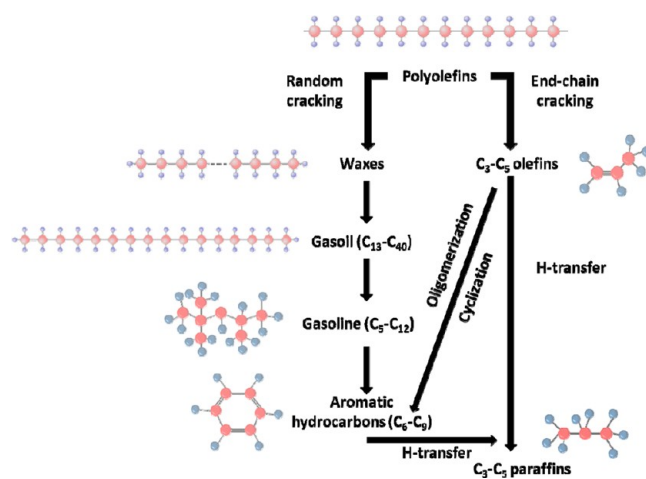


Figure 1. Reaction pathways in the catalytic cracking of polyolefins (reprinted with permission from ref 15, copyright American Chemical Society).

depicts a summary of the different pathways occurring in the catalytic cracking of polyolefins and clearly illustrates the complexity of the system and describes the plethora of products attainable.¹⁵

The main advantages of catalytic cracking versus thermal cracking can be summarized in the following points:

- Catalytic cracking operates at lower temperature, since it reduces the activation energy of the cracking. In this regard, the more active the catalyst, the lower this cracking temperature.¹⁶
- The catalyst allows the selectivity of the plastic conversion to be tailored so it can be targeted toward the desired products (e.g., gases, gasoline, or diesel) just

by choosing adequately the acidity and pore structure of the catalyst.¹⁷ The nature of the obtained products after catalytic cracking is fairly different from that obtained from thermal conversion, since it contains larger amounts of branched, cyclic, and aromatic hydrocarbons. The presence of these sorts of hydrocarbons is positive for the formulation of gasoline (increase in the research octane number (RON) values) and, to some extent, also for diesel (improving the pour and cloud point, although at the expense of lower cetane numbers), provided that enough care is taken not to surpass the legislation limits of the fuels, especially in the case of the aromatics.^{18,19}

Nonetheless, it should be mentioned that there are also significant drawbacks in the catalytic cracking of polymers, which are mostly associated with the inherent nature of the chosen catalyst. Thus, the deactivation of the catalyst is always occurring, and in some cases, the extent and quickness of the deactivation phenomena pose a serious bound to this technology. On the other hand, the activity and selectivity in the catalytic cracking depend largely on the chosen catalyst, and factors such as pore size or acidity wield a decisive influence upon its performance.

One point that should be taken into consideration is the selection of the reaction conditions (e.g., the temperature), since it determines whether the thermal cracking proceeds in an important extent simultaneously to the catalytic cracking. In this case, in addition to the direct catalytic cracking of the polymer, a part of the polymer undergoes thermal cracking, and some of the obtained products might be additionally reformed over the catalyst. Therefore, in some reaction systems, the borderline between thermal and catalytic cracking is difficult to establish.

2. THE ORIGINS OF POLYOLEFIN CATALYTIC CRACKING

The catalysts usually employed for polyolefin cracking contain Lewis or Brønsted acid sites or a combination of both of them. Initially, the first acid catalysts used were homogeneous ones, of the kind of Lewis acids. The most usual Lewis acids thus employed were aluminum trichloride and metal aluminum tetrachloroaluminate melts (e.g., NaAlCl_4 , MgCl_2 , AlCl_3). Ivanova et al.²⁰ obtained a high yield of gases (88.2%) in the catalytic cracking of polyethylene at 370 °C using $\text{MgCl}_2 \cdot \text{AlCl}_3$ as catalyst, isobutane being its main component (42.5%). On the other hand, chloroaluminate ionic liquids, such as 1-ethyl-3-methylimidazolium chloride aluminum(III) chloride, results in the formation of high yields of light C_3 – C_5 alkanes and cycloalkenes after cracking of HDPE, although the addition of a certain amount of a strong Brønsted acid (e.g., sulphuric acid) as cocatalyst was required.²¹ Kaminsky et al.²² used AlCl_3 and also a combination of $\text{AlCl}_3/\text{TiCl}_4$ in the pyrolysis of polypropylene. These catalysts have the initial advantage of being soluble in the polymer at the cracking temperatures (300–500 °C), so they are, indeed, homogeneous catalysts. Hence, unlike what occurs with heterogeneous catalysts, they can be used in lower amounts (<0.1–1 wt %) because of their better contact with the polymer. However, the major problem of these catalysts is their separation from the obtained liquid products, so they are scarcely used. Therefore, heterogeneous catalysts have been the preferred choice in most research works.

Pioneering works of catalytic polyolefin cracking over heterogeneous catalysts dates back to the 1980s. They were

carried out using amorphous silica–alumina, zeolites, and carbons as catalysts. Zeolites are crystalline aluminosilicates whose main feature is the occurrence of a microporous structure. Hence, the micropore size may vary within the 0.4–1.0 nm range, depending on the zeolite topology. In contrast, silica–aluminas are amorphous aluminosilicates whose pore structure usually contains mostly mesopores or macropores (or both) and lacks any crystalline ordering. These differences in pore structure and crystallinity are rather important, since they determine the acid features of the catalysts that control the activity and the selectivity in the catalytic cracking.

The initial studies in the field using these catalysts proved that secondary reactions, such as isomerization and aromatization, took place extensively.^{23,24} Thus, Ishihara et al.²⁵ measured the branchings in the oligomers attained in the polyethylene cracking over silica–alumina in a semibatch reactor. The majority of these branchings were of short length (< C_6), ranging from methyl to pentyl and also including branched alkyl chains, such as 2-ethylhexyl, 2-ethylpentyl, and 2-ethylbutyl. The content of branchings, determined by ^{13}C NMR (Figure 2) increased on decreasing the molecular weight

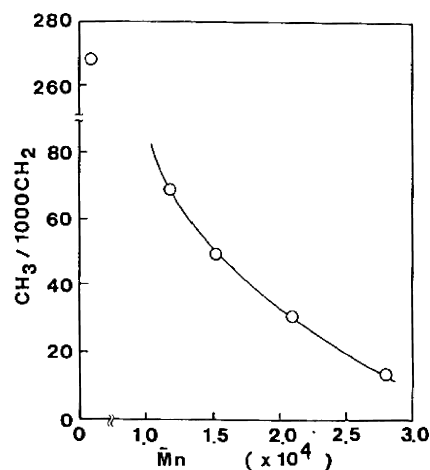


Figure 2. Relation between the reduction of molecular weight of polyethylene after catalytic cracking over silica–alumina and the content of branchings in the degraded products (reprinted with permission from ref 25, copyright John Wiley and Sons).

of the degraded oligomers, reaching a maximum value of 74 per 1000 carbon atoms. On the other hand, these initial studies also indicated that the catalyst played a key role, since it affected the composition of the hydrocarbon mixtures finally obtained. Thus, clear differences were observed between zeolites and amorphous silica–alumina. Vasile et al.^{26,27} detected in the degradation of polyethylene and polypropylene at 450–500 °C higher amounts of gaseous hydrocarbons (in particular, C_4 hydrocarbons) and aromatics (mostly toluene and xylenes) over zeolite ZSM-5 than over silica–alumina. In addition, Beltrame et al.^{28,29} appreciated that the presence of the catalyst lowered both the apparent activation energy of the polyethylene degradation and the frequency factor with regard to pure thermal cracking. However, the effect of the decrease in the activation energy was higher than that of the frequency factor, so the final result was an enhancement of the reaction rate. Thus, the output of gases + liquid distillates collected after reaction was increased. The following order of activity was obtained in the catalytic cracking of polyethylene using a semibatch reactor: zeolite HY > zeolite REY > silica–alumina

(24.2 wt % of alumina) > silica–alumina (13.2 wt % of alumina). These results denoted that zeolites were more active than amorphous silica–alumina.

Activated carbon was also employed for polyethylene cracking at 340–360 °C using a fixed bed flow system, leading to a different product distribution compared with thermal cracking with formation of high amounts of C₁–C₅ *n*-alkanes and C₆–C₈ aromatics.³⁰ However, on the basis of the low yield of branched alkanes and alkenes produced, the mechanism proposed for the catalytic cracking over activated carbons was not of carbocationic but of a radical nature. In this regard, activated carbons promote cyclization reactions, so the hydrogen released in the process saturates the alkenes, giving rise to the high share of alkanes detected. These same authors also observed that the addition of different metals, and especially Pt and Fe, to the activated carbon enhanced the amount of aromatics obtained with regard to metal-free carbon, since the metal catalyzed the slow step of hydrogen desorption in the dehydrocyclization process.³¹ Likewise, the addition of CS₂ to iron supported on activated carbon increased the yield of useful products (naphta, kerosene, and gas oil) in the hydrocracking of propylene at 380 °C in a batch reactor, decreasing meaningfully the amount of residue obtained.³²

Another point of interest identified in the cracking of plastics was the effect of the different additives usually present in the plastics makeup, since it was necessary to ascertain if they might play a catalytic role. In this regard, Ohkita et al.³³ studied the catalytic cracking of the vapors generated from polyethylene thermal cracking in a semibatch reactor over SiO₂, Al₂O₃, ZnO, MgO, and TiO₂, which can be found, for instance, as additives in the polyethylenes manufactured for making electric cables, being employed as flame retardants. Their presence scarcely affected the thermal cracking except for the lower amounts of residue remaining in the reactor, since these compounds worked as scavengers of the radicals formed onto their surface.

4. TYPES OF CATALYTIC REACTORS FOR PLASTICS PROCESSING

Plastic wastes are not conventional reactants, since they have huge viscosities and low thermal conductivities. The plastics viscosity increases with the molecular weight, so the magnitude of mass and heat transfer problems may be significantly different from one polymer to another, since the molecular weight of the polyolefins can vary within the 50 000–1 000 000 g mol⁻¹ range. On the other hand, the polyolefin crystallinity is not expected to exert an effect on polyolefin cracking, since all the crystallites, regardless of the polyolefin, melt at temperatures below 200 °C.

The first catalytic reactors used for cracking of plastics were conventional batch reactors and also fixed beds. However, on using these reactors, both mass and heat transfer constraints appear during the cracking. To solve this problem, fluidized beds were used for the catalytic cracking of plastics, widening the application of the Hamburg process developed initially by Kaminsky for the thermal cracking of plastic wastes.³⁴ Fluidized bed reactors are characterized by possessing a homogeneous temperature and composition throughout the bed, so they seemed to be particularly adequate for the plastic waste cracking. However, the main drawback associated with its usage is the need to employ high amounts of catalysts (polymer to catalysts loads of 6/1 to 1/1) to achieve complete polymer cracking. Otherwise, operation problems may arise, such as the adherence of the unreacted polymer to the reactor walls as well

as the alteration of the free movement of the catalyst particles inside the bed, disturbing the operation of the fluidization regime.³⁵

Owing to this requirement of high amounts of catalysts, the profitability of a polymer cracking process based on fluidized bed reactors requires that the catalyst can be regenerated in a large extent. An especially designed reactor particularly successful for catalytic polyolefin cracking is the conical spouted bed reactor. In this case, the reactor shows a conical shape with a spout inlet for the fluidizing gases. This design has shown some advantages, such as the avoidance of the typical defluidization problems caused by the agglomeration of the sand/catalyst particles coated by melted plastics due to their sticky nature. For conical spouted bed reactors, the vigorous flow of the solid, eased by the spout, allows the formation of agglomerates to be eliminated.³⁶

Another option to decrease the viscosity of the plastic wastes is to dilute them with oils or even Fluid Catalytic Cracking (FCC) feedstocks. In this regard, several authors proposed adding the plastic wastes to the FCC feedstocks and cracking them in conventional FCC units. Thus, riser simulators have been employed for the treatment of plastics wastes/oil hydrocarbon mixtures.³⁷ In addition, Marcilla et al.³⁸ proved the feasibility of this option by cracking a mixture of LDPE–vacuum gasoil with a relative share of LDPE varying within 0–100% range over a equilibrated FCC catalyst in a laboratory fluidized bed reactor reproducing the conditions of FCC units. However, the main problem associated with this option is that the share of plastics in the final mixture to attain a good fluidity should be around 5–10%, since the viscosity increases exponentially beyond this point. On the other hand, when the plastics are added to FCC feedstocks, the possibility of plastics deposition along the pipes and clogging them is also a serious issue that should be taken into account. An interesting solution for this problem was shown by Arandes et al.^{39,40} These authors proposed to carry out first the pyrolysis of the plastic wastes toward waxes in specific plants located on the collection spots. The obtained waxes would be better feedstocks to be fed to the FCC units.

Another type of reactor especially designed to deal with plastic wastes is the screw kiln reactor, which is depicted in Figure 3.⁴¹ The plastics were melted in a hopper at 250–300 °C and fed by a screw into the reaction zone, which was a tube heated externally by two furnaces whose temperatures were independently set (T_1/T_2). The residence time of the plastics might be changed by modifying the screw speed within 0.5–25 rpm. The catalyst was added together with the plastics into the hopper and the mixture of catalyst/plastics was dropped into

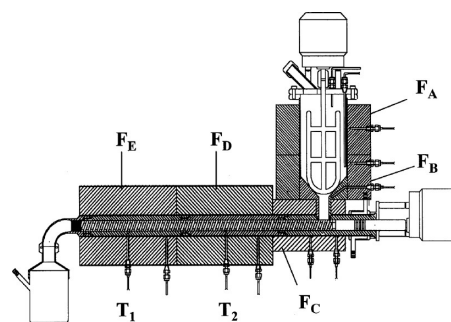


Figure 3. Scheme of the screw kiln reactor (reprinted with permission from ref 41, copyright Elsevier).

the reaction zone. Subsequently, the screw made the catalyst/plastics mixture flow together along the reactor, and the obtained products were recovered at the outlet. The catalyst could be easily removed by filtration of the liquid products. This reaction system has the advantage that the residence time for all the products is the same and allows intimate contact to be achieved between the primary cracking products (gaseous olefins) and the catalyst. Thus, secondary reactions such as oligomerization were favored, since there is no selective removal of the volatile gaseous hydrocarbons, as occurred in semibatch reactors.

Figure 4 compares the results obtained in the thermal cracking of LDPE in a batch reactor and in the screw kiln

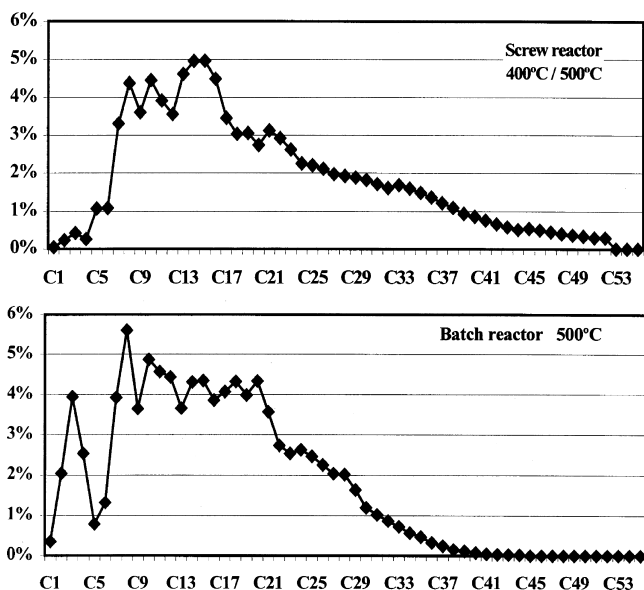


Figure 4. Influence of the type of reactor in the selectivity by atom carbon number obtained in LDPE thermal cracking (reprinted with permission for ref 41, copyright Elsevier).

reactor. It can be clearly observed that the screw kiln reactor originated less gases and increased the amount of heavier hydrocarbons. In this regard, the selectivity toward gasoline obtained in the catalytic degradation of LDPE over Al-MCM-41 catalyst in the screw kiln reactor at 400/500 °C was increased up to 80% with a high yield of C₇–C₈ hydrocarbons (~50 wt %) whose origin was ascribed to the oligomerization of the C₃–C₄ hydrocarbons formed in the primary cracking reactions.⁴¹ Consequently, the adequate choice of the reactor system is also key for determining the finally obtained selectivities.

5. SOLID ACIDS AS CATALYSTS FOR POLYOLEFIN CRACKING

After the aforementioned pioneering works, it was clear that the catalyst was essential to increase both the activity and the selectivity of the catalytic cracking of the polyolefins toward the wanted products. Solid acids turned out to be the most suitable choice, so the number of studies concerning the screening of different catalysts and the investigation of their properties increased considerably. Therefore, the different types of catalysts used as well as the role played by their acidity are discussed below.

5.1. Types of Catalysts for Plastic Processing. The main types of solid catalysts used for the catalytic cracking of plastics are the following: zeolites, silica–alumina, ordered mesoporous aluminosilicates (Al-MCM-41 and Al-SBA-15), clays, and FCC catalysts. The need for an adequate selection of the catalyst was highlighted by Songip et al.,⁴² who performed a screening of catalysts (HY zeolite, rare earth metal-exchanged Y zeolite, silica–alumina, HZSM-5) in catalytic reforming in a fixed bed flow reactor at 400 °C of the oils coming from waste polyethylene pyrolysis. The most suitable catalyst was rare earth metal-exchanged Y zeolite, giving rise to 48% wt of gasoline with a RON number of 67. According to these results, zeolites seemed to be good candidates as catalysts for polyolefin cracking, so different studies were carried out to ascertain the influence of the zeolite pore architecture as well as its acidity.

In this regard, Mordi et al.⁴³ investigated the catalytic cracking of polyethylene at 350 °C over H-mordenite, H- θ -1, and HZSM-5 zeolites in a batch reactor and found that HZSM-5 gave rise to products lighter than C₁₄, but over the other two zeolites, hydrocarbons within C₁₁–C₁₉ were detected. In addition, over HZSM-5, higher amounts of gases (54%) and aromatics (16.8%) were obtained. This difference was ascribed to the occurrence of 10-membered ring sinusoidal and straight intersecting channels in the HZSM-5 zeolite. Interestingly, these authors also pointed out that the cracking initiation took place over the external surface of the zeolite or at the pore mouth, since the polymer is too large to enter the pores. These starting degradation products were subsequently converted over the catalyst through secondary reactions, giving rise to the reported selectivities. On the other hand, zeolite Beta showed higher selectivity than HZSM-5 toward gasoline (60–70%) in the catalytic cracking of LDPE, HDPE, and PP at 400 °C in a semibatch reactor due to its larger pore size (12 rings 0.55 × 0.55 and 0.76 × 0.64 nm channels) and lower acid strength.⁴⁴

Manos et al.⁴⁵ carried out a more thorough study of the influence of the zeolite structure in the catalytic cracking of HDPE at 360 °C in a semibatch reactor. Their study encompassed the following zeolite structures: HY, USY, Beta, H-mordenite, and HZSM-5. They found that the share of lighter products decreased according to the following order: HZSM-5 > H-mordenite > Beta > Y > USY. This means that larger-pore-size zeolites yielded heavier hydrocarbons than medium-pore-size zeolites. In addition, the share of double bonds decreased following the same trend, whereas the alkanes were mostly isoparaffins. Therefore, the pore size architecture plays a key role in the attained olefins/paraffins ratio, since bimolecular hydrogen transfer reactions, responsible for the formation of saturated hydrocarbons and coke, are hindered over the 10-membered ring of zeolite HZSM-5. However, over USY zeolite, possessing 12-membered ring channels (0.74 nm) as well as large cavities, the formation of paraffins and coke takes place easily.

It is noteworthy that some zeolites gave rise to high yields of aromatics; in particular, HZSM-5 and HY. In this regard, Bagri et al.⁴⁶ observed in the catalytic cracking in a fixed bed reactor of the gaseous product from the polyethylene thermal pyrolysis at 500 °C that the share of aromatics was much higher in oils produced with HY zeolite than in the oils from HZSM-5 (37.2 vs 7.69% at 600 °C). Over HY zeolite, these aromatics were largely single ring aromatics (toluene and ethylbenzene, 24.34%), although a significant amount of polycyclic aromatics (4.54%) was also formed (mostly two-ring aromatics, such as naphthalene, phenanthrene, and pyrene derivatives). Similar

conclusions were drawn by Hernández et al.⁴⁷ in the catalytic flash pyrolysis of HDPE in a fluidized bed reactor.

One important fact observed in the experiments with zeolites was that it seems to be a limit in the decrease of the cracking temperature in the thermogravimetric experiments that may be accomplished by the increase in the amount of catalyst.⁴⁸ This was shown in the thermogravimetric degradation of HDPE/USY mixtures ranging from 1:1 to 9:1 since the onset temperature for degradation decreased from 500 °C with no catalyst loading to roughly 257 °C for the ratios 1:2, 1:1, or 2:1, which were very similar.

Zeotypes were also evaluated for the polyolefin cracking and showed promising results. In this regard, Fernandez et al.⁴⁹ assessed the performance of the silicoaluminophosphate SAPO-37, possessing the Faujasite structure (the same as zeolite Y), for the thermogravimetric degradation of HDPE. The presence of the catalyst decreased the apparent activation energy from 290 kJ mol⁻¹ (thermal cracking) to 220 kJ mol⁻¹ (with SAPO-37), resulting in lighter products within the C₂–C₁₂ range, which was ascribed to its respective channel architecture.

Several groups investigated the behavior of natural zeolites for the catalytic cracking of polyolefins, since they are cheaper than synthetic ones. Although clinoptilolite showed certain catalytic activity, this was much lower than synthetic zeolites.^{50,51} Hwang et al.⁵² treated the clinoptilolite with boric acid and phosphoric acid to increase their respective BET surface area and pore volume and used it in the catalytic degradation of PP at 400–450 °C in a semibatch reactor, leading mostly to C₄–C₁₂ hydrocarbons. The acid treatment of the clinoptilolites with boric acid and phosphoric acids shifted the product carbon distribution to lower atom carbon numbers because of the more extensive cracking as a consequence of their larger BET surface areas and pore volumes.

Amorphous silica–alumina was initially used for the catalytic cracking of polyolefins. This catalyst showed lower activities than zeolites due to its weaker acidity. In this regard, Aguado et al.⁵³ observed in the catalytic cracking of PP, LDPE, and HDPE over silica–alumina in a semibatch reactor that the presence of branches in the polymer backbone brought about the formation of tertiary carbocations, which were more stable, and facilitated the polymer cracking. Thus, the following order of activity among the polymers was recognized: PP > LDPE > HDPE, in agreement with the decreasing amount of branchings present in the polymers. Uddin et al.⁵⁴ also reached a similar conclusion in the catalytic degradation over silica–alumina at 430 °C of HDPE, LDPE, LLDPE, and cross-linked polyethylene (XLPE) in a batch reactor. They found that the catalytic degradation of LDPE and LLDPE occurred in shorter times than that of HDPE and XLPE, bearing out that the structure of the polymer influences the measured cracking rates. Thereby, although the presence of branchings eases the catalytic cracking of the polymer as a result of the formation of tertiary carbocations, the existence of cross-linkings reduced the cracking rates, likely because of steric hindrances to accede to the acid sites for the more rigid polymer structure or to secondary reactions, which originate additional cross-linkings during the cracking.

Garforth et al.⁵⁵ studied the catalytic cracking of HDPE over amorphous SiO₂–Al₂O₃ (SAHA) and compared it with several zeolites (HZSM-5, H-MOR, and HUSY) in a fluidized bed reactor at 290–430 °C. The obtained products were mostly C₁–C₈ hydrocarbons and coke. The corresponding yields of the former are depicted in Figure 5. Both SAHA and USY gave rise to the broadest C₃–C₈ hydrocarbon distribution.

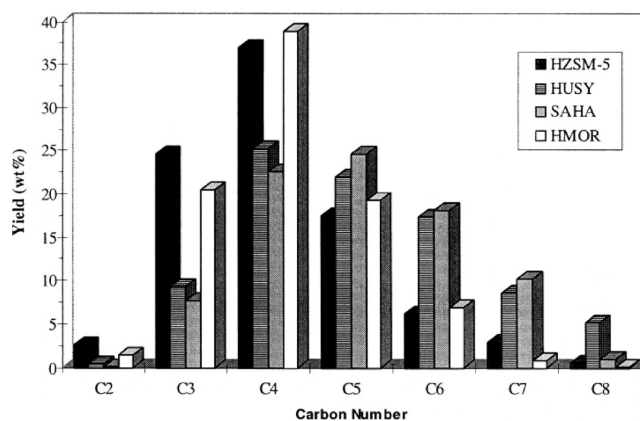


Figure 5. Yields obtained in the catalytic cracking of HDPE at 360 °C in the fluidized bed reactor over different catalysts ($T = 360$ °C, polymer-to-catalyst mass ratio = 40% wt/wt, rate of fluidization gas = 570 mL/min) (reprinted with permission from ref 55, copyright Elsevier).

Interestingly, meaningful differences in the olefins/paraffins ratio were detected between silica–alumina and zeolites. Hence, the silica–alumina, because of the presence of mesopores ($D_p \sim 3.1$ nm) and weak Lewis acid sites, originated high amounts of olefins (ratio olefins/paraffins = 8.6). In contrast, the ratio of olefins/paraffins decreased for the zeolites in the order HZSM-5 (o/p = 2.9) > HMOR (o/p = 1.5) > HUSY (o/p = 0.5) as a result of the predominant presence of strong Brønsted acid sites over these zeolites, which favors bimolecular hydrogen transfer reactions.

The possibility of combining sequentially zeolites and silica–alumina to enhance its individual performance was explored by Uemichi et al.⁵⁶ in the catalytic cracking of polyethylene. They found that if silica–alumina and HZSM-5 were placed sequentially in a fixed bed tubular reactor using a 9/1 mass ratio, high yields of gasoline (58.8%) were attained with a RON of 94, with the amount of aromatics at 25.2%, and benzene, only 0.9%. The low amount of HZSM-5 used avoided the formation of excessive amounts of aromatics, whereas the cause of the high RON value was the large isomerization, which brought about a great deal of isoparaffins.

Ordered mesoporous aluminosilicates (Al-MCM-41, Al-SBA-15) were reported for the first time in 1996 for polyolefin cracking and showed remarkable results.⁵⁷ These catalysts are characterized by a uniform mesoporosity, which can be tailored within the range 1.5–30.0 nm by choosing properly the synthesis conditions. The mechanism proposed for the formation of these ordered mesoporous aluminosilicates is based on the growth around micelles.^{58,59} These micelles aggregate into hexagonal structures that work as templates, so the silica entities condense around them. Subsequently, the template is removed by calcination, releasing the ordered mesoporous structure.

Unlike the zeolites, the pore walls in ordered mesoporous aluminosilicates are not crystalline, so they lack the high hydrothermal stability of the zeolites. Figure 6 displays the TEM micrograph of an ordered SBA-15 material wherein its uniform mesoporosity may be clearly seen.⁵⁹ The presence of a high surface area in Al-MCM-41 (~ 1000 m² g⁻¹), as well as the occurrence of uniform mesopores (2.7 nm), resulted in higher conversions than amorphous SiO₂–Al₂O₃, despite their similar medium acid strength distribution.⁵³ This effect of accessibility

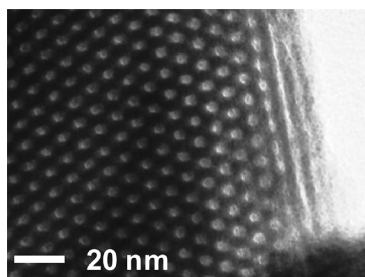


Figure 6. TEM micrograph of an ordered SBA-15 mesoporous material (reprinted with permission from ref 59, copyright Gabriel Morales).

of the acid sites was especially denoted in the catalytic cracking of PP over Al-MCM-41 and HZSM-5. With the former, 99% conversion was attained, whereas over the zeolite, just 11.3% was obtained, since the polymer cannot access the acid sites located in the zeolite micropores because of the steric hindrance posed by the methyl moieties of the PP backbone. The only accessible ones are those present over the outer surface.

The same conclusions were drawn by Garforth et al.⁶⁰ in their thermogravimetric experiments of catalytic degradation of HDPE over HZSM-5 and HMCM-41 samples wherein similar degradation rates were detected, despite their inherent different acid strengths. The proposed explanation was the presence of uniform mesopores with a size of roughly 5.0 nm over the Al-MCM-41 catalyst, which enables improved accessibility of the polymer toward the acid sites. Likewise, this enhancement in activity was also observed with other mesoporous materials, such as Al-UTD-1.⁶¹ This catalyst showed mesoporosity with 3D connectivity and mesopores within 2–50 nm, although the mesopore surface area ($\sim 200 \text{ m}^2 \text{ g}^{-1}$) was considerably lower than that of MCM-41 ($\sim 1000 \text{ m}^2 \text{ g}^{-1}$); however, it was enough to provide lower apparent activation energies than that corresponding to USY zeolite.

Aguado et al.⁶² discovered that the synthesis method of the mesoporous material was key for their catalytic properties. Hence, the catalytic performance of different mesoporous materials, such as Al-SBA-15 and Al-MCM-41 prepared by a hydrothermal method (Al-MCM-41_{hy}) and Al-MCM-41 synthesized by a sol–gel method (Al-MCM-41_{sg}), were tested in the catalytic thermogravimetric degradation of pure HDPE, LDPE, and waste plastics from urban and agricultural origin. Figure 7 depicts the TG and DTG analyses obtained in the catalytic degradation of LDPE over different catalysts. Al-SBA-15 differed from the MCM-41 samples in having a higher mesopore size (4.3 nm vs 2.2–2.4 nm of Al-MCM-41) and lower BET surface area ($496 \text{ m}^2 \text{ g}^{-1}$). In addition, all these catalysts, despite containing close Si/Al atomic ratios (~ 37 – 52), showed different acid strengths, which varied according to the next sequence Al-MCM-41_{hy} > Al-MCM-41_{sg} > Al-SBA-15. With pure polymers, the Al-MCM-41_{hy} showed the highest activity as a result of the stronger acid strength, and Al-SBA-15 displayed better performance than Al-MCM-41_{sg} likely because of its higher pore size. However, when using waste polymers, only Al-MCM-41_{hy} led to considerably higher activities because it presented the stronger acidity among the mesoporous materials. The waste polymers were more difficult to degrade catalytically because of several factors, such as the presence of impurities (potential catalyst poisons and promoters of the formation of coke) or polymer cross-linking caused by either

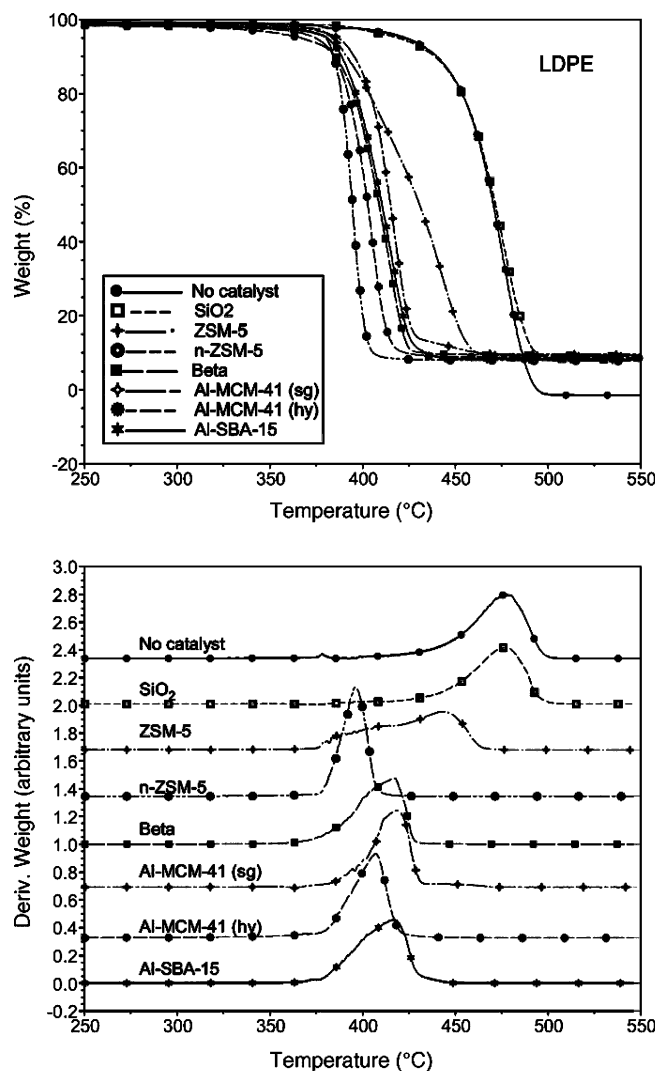


Figure 7. TG and DTG analyses describing the degradation of LDPE over different acid catalysts (reprinted with permission from ref 62, copyright Elsevier).

the usage of or being subjected to the action of environmental factors. Therefore, with waste polymers, strong acidity was required for the catalytic degradation of the polyolefin.

Other materials tested for the catalytic cracking of polymers were clays and pillared clays. These materials are characterized by having a layered structure. The voids between the layers can be enhanced by intercalating different moieties, such as metal oxides (pillaring) originating micropores larger than those existing in zeolites. Clays and pillared clays (smectite and montmorillonite) gave rise to higher yields of liquids ($\sim 70\%$) than USY zeolite ($\sim 50\%$) in the catalytic cracking of polyethylene at 300–400 °C in a semibatch reactor,⁶³ with gasolines being the main components. The weaker acidity of the clays avoided the overcracking toward smaller molecules observed with the USY zeolite. In addition, the extent of bimolecular hydrogen transfer reactions was much lower with the clays, leading to higher amounts of alkenes in the oils as well as lower coke levels than with the USY zeolite. It is also noteworthy that the pillared clays and their original clays gave similar performance, so no influence was observed after the variation of the pore size of the clays by pillaring. However, after the regeneration by combustion of the coke, the pillared

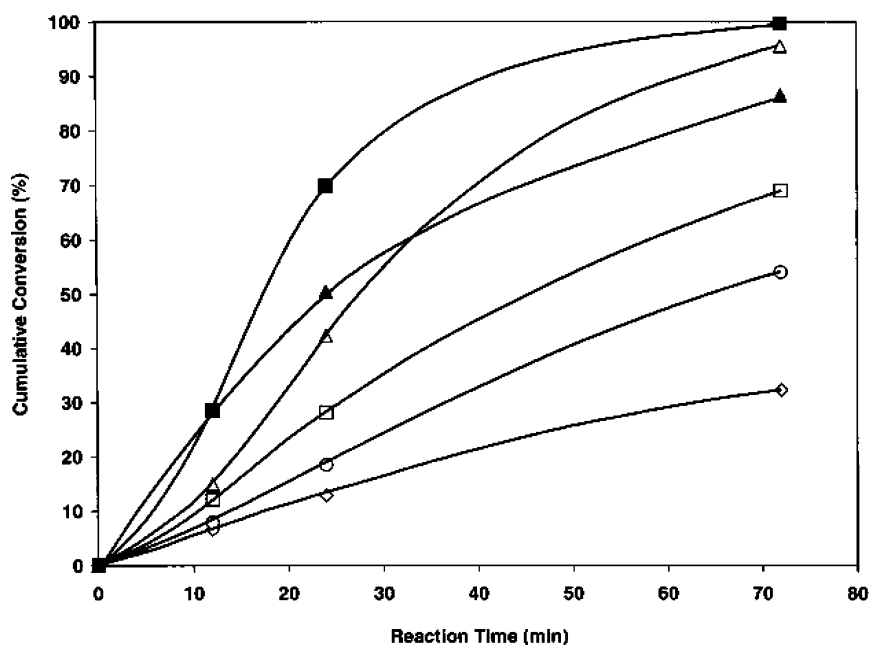


Figure 8. Catalytic cracking of PP at 380 °C over different catalysts: Resor-g (◇ 1 g; ○ 1.5 g; □ 1.75 g; △ 2 g). Si–Al (13%, ■) and USY (▲) were introduced for comparison (plastic/catalyst mass ratio of 35/1.5) (reprinted with permission from ref 65, copyright Elsevier).

clays hold practically the same conversion and product distribution, but the nonpillared clays were more prone to collapse, thereby changing the reported yields.⁶⁴

On the other hand, FCC catalysts were proposed as feasible catalysts for the catalytic cracking of polymers.^{34,65–71} Figure 8 shows the performance in the catalytic cracking at 380 °C of polypropylene in a semibatch stirred reactor of several solid acids: silica–alumina (13%), used equilibrium FCC catalyst (Resoc-g), and USY zeolite. Although the activity of the used equilibrium FCC catalyst was lower than that of the other acid solids, it was considered interesting because of its negligible cost.⁶⁵ Arandes et al.³⁷ appreciated that the equilibrated FCC catalysts after successive cycles of reaction-regeneration possessed considerably less BET surface area (342 vs 175 m² g^{−1}) and acidity (0.42 vs 0.017 mmol NH₃ g^{−1}) than the fresh catalyst. This difference explained, in the catalytic cracking of 5 wt % polyolefin/95 wt % refinery vacuum gasoil mixtures in a riser simulator, the higher conversions obtained over the fresh catalyst (35% vs 20%) with a parallel enhancement in the amount of coke (18% vs 6%). In addition, the use of equilibrated FCC catalysts poses some doubts regarding the presence of heavy metals such as Ni or V. In this regard, Salmiaton et al.⁶⁸ observed in the catalytic cracking of HDPE over equilibrated catalysts in a fluidized reactor containing up to 5400 ppm of Ni and 6580 ppm of V a considerable loss of activity, largely increasing the portion of alkenes (~80%) with regard to fresh and also steamed FCC catalysts without heavy metals.

Likewise, other aspect to be considered in the usage of plastics added to FCC streams is the amount of coke generated, since it is necessary to fulfill the FCC heat balance. In this regard, de la Puente et al.⁷² found that the addition of 10% of plastics to the FCC streams fed to a riser simulator increased slightly the coke content of the catalysts (5.7% vs the average 5% in FCC). However, the coke yields are within reasonable operating margins of the FCC units. On the other hand, it is also worth mentioning that a synergy effect was found in the catalytic degradation at 510 °C of HDPE dissolved in vacuum

gasols (5–10 wt %) using a FCC catalyst. The conversion and the gasoline yields were enhanced with regard to the catalytic cracking of pure vacuum gasoil.⁷³ Similar findings were attained by Arandes et al.⁷⁴ in catalytic cracking at 500–550 °C in a riser simulator reactor of the hydrocarbon mixtures formed by vacuum gasoil and waxes obtained in the flash pyrolysis of PP. The higher conversion and yields of gasoline attained when the waxes were added to the vacuum gasoil was ascribed to their higher reactivity, since their makeup contained high amounts of olefins, unlike the vacuum gasoil, wherein aromatics were the main component.

5.2. Acidity. The catalyst acidity, in terms of type, strength, and amount, exerts a deep influence on the catalytic performance, since it determines the activity and the selectivity of the catalysts. The presence of aluminum, responsible for the zeolite acidity, is crucial to showing activity, since, for instance, silicalite (ZSM-5 zeolite without aluminum in its makeup) exhibited hardly any activity for the conversion of HDPE at 360 °C in the fluidized bed reactor.³⁵ The activity of the catalysts increases with their acid strength, provided that no steric or diffusional hindrances are occurring. In this regard, Zhao et al.⁷⁵ observed by thermogravimetry in the catalytic cracking of polypropylene that the activity dropped following the order HY > H-mordenite > H-L zeolite > Na-mordenite which is in keeping with the acid strength of the catalyst. However, in this study, the effect of the catalyst structure could not be separated from those of the acid strength.

In addition to the acid strength, the number of acid sites also affects the activity and the selectivity in the polymer cracking. The number of acid sites may be easily augmented by increasing the amount of catalyst used or by decreasing the Si/Al atomic ratio of the catalyst. In this regard, Ohkita et al.³³ observed in the catalytic cracking of the volatile products coming from the polyethylene thermal cracking over silica–alumina at 400 °C in a semibatch reactor that an increase in the acid content of the catalysts enhanced the amount of gases and diminished the content of oils. In agreement with this statement, Akpanudoh et al.⁷⁶ detected a relationship between

the acid content and the amount of oils produced in the catalytic degradation of LDPE at 377–417 °C in a semibatch reactor using two commercial FCC catalysts containing 20 and 40 wt % of zeolite USY. They obtained the graph of liquid yields versus acidity depicted in Figure 9 wherein a clear

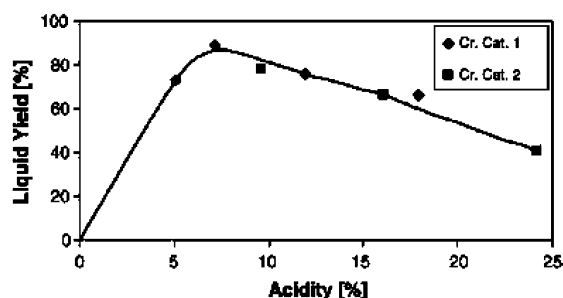


Figure 9. Liquid yields versus acidity obtained in the catalytic cracking of LDPE at 650–690 K using two commercial FCC catalysts and varying the polymer-to-catalyst mass ratio within 1/1–1/6 (reprinted with permission from ref 76, copyright Elsevier).

maximum for a 7% content of zeolite USY was detected. Therefore, the excess of zeolite (and of acidity) clearly promotes overcracking of the liquids, creating more gaseous products.

On the other hand, Neves et al.⁷⁷ found by thermogravimetry and DSC that in the catalytic degradation of polyethylene using three dealuminated HY zeolites with Si/Al atomic ratios varying from 2.8 to 13.0 that the apparent activation energies decreased on enhancing the Si/Al atomic ratios. The higher activity observed in the samples with lower aluminum content was ascribed to the presence of more isolated Brönsted acid sites, which are expected to show stronger acidity. Likewise, Elordi et al.⁷⁸ observed in the catalytic cracking of HDPE at 500 °C in a conical spouted bed reactor over HZSM-5, agglomerated with bentonite and inert alumina, that on increasing the SiO₂/Al₂O₃ ratio from 30 to 80, the portion of nonaromatic C₅–C₁₁ hydrocarbons was enhanced (from 15.5 to 25.4 wt %) while in parallel, the yields of monoaromatics and light alkane fractions (<C₄) decreased.

The acid strength of the zeolite, controlled by the SiO₂–Al₂O₃ ratio and the nature of the counterion (Na⁺, low acidity; H⁺, high acidity), is a key factor for obtaining high activity in the polyolefin degradation. In keeping with this, sulfated zirconia, an extremely strong acid solid, showed higher activity in polyethylene degradation by thermogravimetry than both HZSM-5 zeolite and silica–alumina.⁷⁹ Coelho et al.⁸⁰ highlighted this point by varying the zeolite acidity by means of the incorporation of different amounts of Na⁺ ion inside the HZSM-5 zeolite. It was detected by thermogravimetry in the catalytic pyrolysis of polyethylene that higher amounts of sodium decreased the acidity, resulting in parallel in the enhancement of the temperature of polyethylene cracking from 402 to 465 °C. Likewise, Neves et al.⁸¹ also tailored the acidity of HY and NaY zeolites by ion exchange with NaNO₃ and NH₄NO₃, respectively, obtaining intermediate cracking rates in the thermogravimetric degradation of HDPE over these catalysts, with regard to pure NaY and HY zeolites. These results emphasize that strong acidity was especially effective for the polymer cracking, but the role played by the weak acid sites was not clarified. In this regard, Songip et al.⁸² performed catalytic degradation of the heavy oil obtained from the thermal

pyrolysis of polyethylene over rare earth metal-exchanged zeolite Y in a fixed bed reactor, setting up a kinetic model for their degradation into four lumps; gas, gasoline, heavy oil, and coke. They appreciated that the attained kinetic constants for each lump fitted rather well with the content of strong acid sites of this catalyst but not with either the total amount of them or the amount of weak acid sites and concluded that the strong acid sites were the ones effective for the cracking.

On the other hand, the acid strength of the catalyst determines not only the activity but also the attained selectivities. This was clearly shown by Aguado et al.⁵³ in the catalytic cracking of LDPE, HDPE, and PP over SiO₂–Al₂O₃, Al-MCM-41, and HZSM-5 at 400 °C in a semibatch reactor. Over HZSM-5, the selectivity was addressed mostly toward gases (C₁–C₄, roughly 45–50%) because of its high acid strength, regardless of the polymer. In contrast, over SiO₂–Al₂O₃ and Al-MCM-41, gasoline (C₅–C₁₂ hydrocarbons, roughly 50–65%) and gasoils (C₁₃–C₂₂, around 10–30%) were the major products because of their medium acid strength. The reason for the higher selectivity toward gases with strong acid catalysts is because they promote an end-chain cracking mechanism of the polymer backbone. In contrast, over medium acid strength catalysts, a random-chain cracking mechanism takes place, meaningfully originating a far higher amount of middle distillates (C₁₃–C₂₂). These differences can be additionally demonstrated in Figure 10, which depicts the selectivity by carbon atom number attained in PP cracking at 400 °C over HZSM-5, SiO₂–Al₂O₃, and Al-MCM-41.

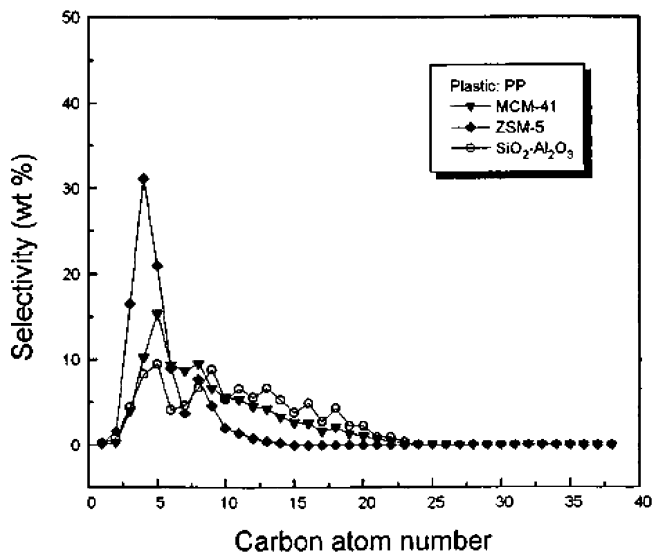


Figure 10. Selectivity by atom carbon number obtained in the catalytic cracking of PP (400 °C, 0.5 h, plastic/catalyst mass ratio = 36/1) (reprinted with permission from ref 53, copyright American Chemical Society).

Another aspect of interest is the relative amount of Brönsted and Lewis acid sites, since the former are known to be more active for the polyolefin cracking and also may lead toward different selectivities. The ratio of Brönsted to Lewis acid sites in the catalyst may be changed by adding heteroatoms different from Al into its structure. In this regard, the introduction of Ga into the zeolite framework seems a rather feasible choice to attain high amounts of aromatics, which are valuable chemicals. Thus, the presence of gallium instead of aluminum in the zeolite results in a H-gallosilicate which showed remarkable

selectivity to aromatics in the catalytic degradation of low density polyethylene at 375–550 °C using both a fixed bed flow reactor and batch reactors. Thus, BTX selectivities (BTX: benzene + toluene + xylenes) of 58% were detected at 500 °C over this gallosilicate.⁸³ Likewise, Zn was incorporated by ion exchange into the HZSM-11 zeolite, causing a huge enhancement of the content of Lewis acid sites (the Lewis/Brønsted ratio was 3.53 for Zn-ZSM-11; for HZSM-11, it was just 0.09).⁸⁴ This difference gave rise to more liquids with a high amount of aromatics (up to 96%) over Zn-ZSM-11 in the catalytic cracking of LDPE at 500 °C in a fixed bed tubular reactor.

5.3. Deactivation. The deactivation of the catalyst is another key aspect for assessing the performance of the catalytic cracking of plastics. The different literature studies carried out up to now stress that the deactivation resistance depends strongly not only on the acidity but also on the pore structure of the catalyst. In this regard, Uemichi et al.,⁸⁵ in the catalytic degradation of polyethylene at 375–526 °C over silica–alumina, HZSM-5, H-mordenite, and HY in a fixed bed, determined the amounts of coke deposited vs time (Figure 11).

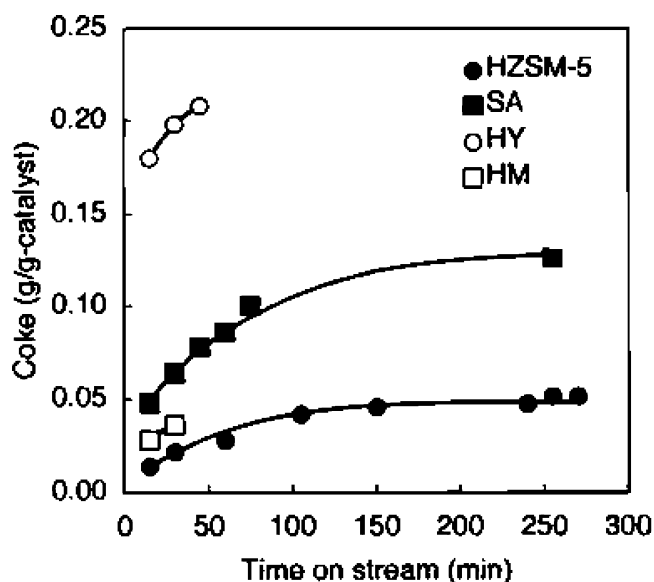


Figure 11. Amounts of coke deposited over the catalysts (○, zeolite HY; □, zeolite H-mordenite; ■, silica–alumina; ●, zeolite HZSM-5) with time on-stream at 450 °C (reprinted with permission from ref 85, copyright American Chemical Society).

They observed that H-mordenite and HY deactivated quickly, and HZSM-5 and silica–alumina were hardly deactivated. It is noteworthy that silica–alumina was deactivated less than expected according to the high amounts of coke deposited because of the occurrence of larger mesopores (2–8 nm), which allow the reacting molecules to diffuse, despite the coke present. H-mordenite, despite having low amounts of coke deposited, quickly lost its activity due to the blocking of its unidimensional channels. For the case of HY zeolite, instead, the deactivation was caused by the filling of its channels and cages with coke.

Ali et al.⁸⁶ also measured the amount of coke deposited over different catalysts in the catalytic degradation of HDPE at 450 °C in a fluidized bed reactor. It decreased according to the following order: fresh FCC catalyst (13.3%) > USY zeolite (9.7%) > silica–alumina (5.0%) > ZSM-5 (2.4%) > equilibrated FCC catalysts (1.9–1.5%). For the case of the USY zeolite, Lin

et al.⁸⁷ discovered that the activity dropped exponentially with the coke content in thermogravimetric experiments. Nonetheless, Lin et al.⁸⁸ also found that in the case of FCC equilibrium catalyst, it could be regenerated up to four times by heating under air to 520 °C, so the catalyst recovered most of its initial activity, and the main slight loss in activity was placed during the first regeneration treatment.

Elordi et al.⁸⁹ found in the catalytic pyrolysis of HDPE at 500 °C in a conical spouted bed reactor using zeolites HY, HBeta, and HZSM-5 that the latter was the catalyst that underwent the lowest deactivation, showing lower micropore blockage and lower reduction in acidity. HZSM-5 was resistant to deactivation due to the steric hindrance posed by their pore structure (0.53 × 0.56 nm straight channels and 0.51 × 0.55 nm sinusoidal channels) for the growth of the bulky coke intermediates. Lin et al.⁹⁰ also bore out that HZSM-5 deactivated less than HMCM-41 and silica–alumina in the catalytic cracking of HDPE in a fluidized bed reactor. Thus, the share of isobutane and isopentane, which are formed as a result of bimolecular reactions, decreased with time whereas the amount of olefins, formed in monomolecular reactions, was enhanced over HMCM-41 and silica–alumina. Instead, over HZSM-5, their respective share remained virtually unchanged.

Marcilla et al.⁹¹ studied more deeply the deactivation behavior of HZSM-5 zeolite, carrying out several cycles of catalytic cracking of LDPE and HDPE in a batch reactor. According to this work, the deactivation performance of HZSM-5 depends on the used polyolefin. Thus, after just one cycle with HDPE, the catalyst showed a product distribution similar to thermal cracking, whereas with LDPE, four cycles were required to appreciate a partial loss in activity. This was due to the faster growth of coke inside the HZSM-5 zeolite with HDPE than with LDPE. Hence, BET surface areas values decreased, reaching values of 217 and 91 m² g⁻¹ after the first cycle (the starting one was 341 m² g⁻¹) with LDPE and HDPE. In this regard, ZSM-11 zeolite displayed a remarkable performance after successive cycles of LDPE cracking, since this zeolite was able to hold its activity after eight reaction cycles (see Figure 12) because of its medium pore size.⁹² The steric constraints hindered the bimolecular reactions such as hydrogen transfer and condensation, which are responsible for the formation of the bulky, highly condensed molecules of

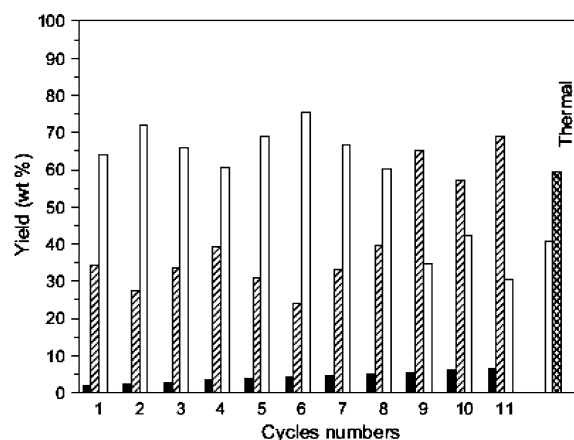


Figure 12. Performance of the HZSM-11 zeolite after successive reactions cycles in the cracking of LDPE (plastic/catalyst mass ratio of 2/1; $T = 500$ °C) (reprinted with permission from ref 92, copyright Elsevier).

coke, so they occur more slowly than over, for example, Beta zeolite.

Marcilla et al.⁹³ also studied the nature of the coke deposited over HZSM-5 and HUSY after the catalytic cracking of LDPE in a tubular fixed bed reactor. They found that the higher the cracking temperature (450–750 °C range), the lower the amount of coke deposited over these catalysts. In the case of HZSM-5 zeolite, the coke was mostly located within the micropores, although on increasing the cracking temperature, a certain amount (<10 wt %) moved out toward the external surface. Likewise, the coke obtained at higher cracking temperatures showed a larger share of insoluble coke in dichloromethane assigned to more bulky species, chiefly polyaromatic compounds, which is the cause of the higher temperatures required for their elimination in the TGA experiments. On the other hand, Castaño et al.⁹⁴ observed that the aromatic condensation degree of the coke obtained in the catalytic cracking of HDPE over HZSM-5, HY and HBeta in a conical spouted bed reactor increased with the pore size, so the coke formed over HZSM-5 showed a higher concentration of aliphatics than those attained over HY or HBeta zeolite.

Castaño et al.⁹⁵ also studied the mechanism of coke formation over a HZSM-5 zeolite agglomerated with bentonite and α -Al₂O₃ in the cracking of HDPE and PP at 500 °C in a conical spouted bed reactor. They detected that the strong acid sites were the first to disappear after the deposition of around 2 wt % of coke, but the amount of weak acid sites was scarcely affected by the coke deposition. In addition, they distinguished two stages in coke formation: (1) initiation and (2) steady deactivation. The first one gave rise to so-called “coke II”, mostly aromatic and located inside the micropores, whereas during the second stage, “coke I” was formed instead, with a size greater than the zeolite pore, so it was placed mostly on the outer surface and contained higher amounts of aliphatics.

The presence of poisons in the reaction medium should also be taken into account in the catalytic cracking of plastic wastes, since special provisions should be made for them. This was shown by Serrano et al.⁹⁶ in the catalytic cracking of mixtures of LDPE–lube oil in a screw kiln reactor, since the lower reactivity of the lube oil and also the presence of considerable amounts of sulfur (4000 ppm) and nitrogen (85 ppm) into its makeup led to lower activities than in the cracking of the pure LDPE. Both negative effects were overcome by increasing the reaction temperature to 450/500 °C (reaction zone 1/reaction zone 2), which enhanced the activity of the acid sites and lowered the chemisorption strength of the nitrogen- and sulfur-containing compounds. On the other hand, Wei et al.⁹⁷ carried out the catalytic cracking of waste plastics (~40 wt % HDPE + 27 wt % LDPE + 33 wt % PP) containing 0.23% of N and 0.07% of S in a fluidized bed reactor over different acid catalysts (USY, HZSM-5, H-mordenite, silica–alumina, and MCM-41). The presence of these heteroatoms was not a problem for the catalytic cracking. In addition, the obtained C₁–C₉ hydrocarbons (yield >80 wt %) did not contain sulfur in their makeup, which was a positive feature, considering the future application of these hydrocarbons.

Another point that must be taken into account in the catalytic cracking of plastic wastes is the possible presence of polystyrene in the raw residues. In principle, this polymer is easily separated by flotation from the plastic waste stream, so its occurrence should be decreased to practically null. If not, deactivation problems might arise, since the thermal cracking of this polymer generates huge amounts of aromatics (especially

styrene), which are known as coke precursors. Thus, de la Puente et al.⁹⁸ obtained considerable amounts of coke (above 30 wt %) in the cracking of polystyrene over FCC catalysts at 550 °C in a discontinuous fluidized bed reactor. On the other hand, Serrano et al.⁹⁹ found fairly low cracking activity in the degradation of polystyrene at 375 °C in a semibatch reaction over HZSM-5, since in this case, the high acid strength of the zeolite promoted mostly cross-linking reactions within the polymer backbone, creating the formation of another polymer, instead of the cracking products. Consequently, the presence of high amounts of polystyrene making up the plastic waste composition might be detrimental for an effective catalytic cracking to proceed.

5.4. Mechanistic and Kinetic Considerations. An important aspect for the application of the catalyst to an industrial process is the kinetic modeling of its performance. To facilitate kinetic modeling, the reaction products are usually grouped in different lumps. In this regard, Ding et al.¹⁰⁰ in their thermal pyrolysis experiments of HDPE and mixed plastics in a batch reactor set up four lumps—light fractions (L), middle distillates (M), heavy fractions (H), and polymers (P)—and proposed the reaction mechanism shown in Figure 13. The

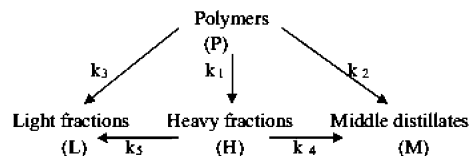


Figure 13. Reaction mechanism in the thermal pyrolysis of polyolefins (reprinted with permission from ref 100, copyright Elsevier).

authors put forward several assumptions for this reaction mechanism: (1) all the reactions were first-order and referred to the mass fraction of the lumps, (2) all the reactions were irreversible, (3) mass and heat transfer resistance were considered negligible, (4) the temperature dependence of the rate constant was described by the Arrhenius law, and (5) the polymers in the autoclave were considered unreacted during the heat-up period. The obtained activation energies for the conversion of HDPE to heavy fractions, middle distillates, and light fractions were 219.11, 198.54, and 259.19 kJ mol⁻¹, and the pre-exponential factors were 3.70×10^{15} , 1.20×10^{13} , and 3.17×10^{17} min⁻¹, respectively. Interestingly, the model provided good fitting for k_1 , k_2 and k_3 constants, but in the cases of k_4 and k_5 , these constants did not show a linear dependence with temperature, suggesting that secondary cracking reactions were not first-order.

Yang et al.¹⁰¹ also proposed a similar four-lump kinetic model for the catalytic degradation of postconsumer polymer waste (PE/PP) in a fluidized reaction system similar to FCC units using as catalyst a commercial FCC equilibrium catalyst (ECat-F1), silica–alumina, and ZSM-5 zeolite. The model comprised four lumps—gases, gasoline, coke, and unconverted polymer—and incorporated an exponential decay function to describe the deactivation of the catalyst. The proposed model fitted rather well the experimental data, describing the effects of temperature and particle size in the reported product selectivities.

On the other hand, Lin et al.¹⁰² proposed a kinetic model for the catalytic degradation of comingled plastics (~38 wt % HDPE + 24 wt % LDPE + 34 wt % PP + 3 wt % PVC + 1 wt % PS) in a fluidized reaction, described in Figure 14. In this

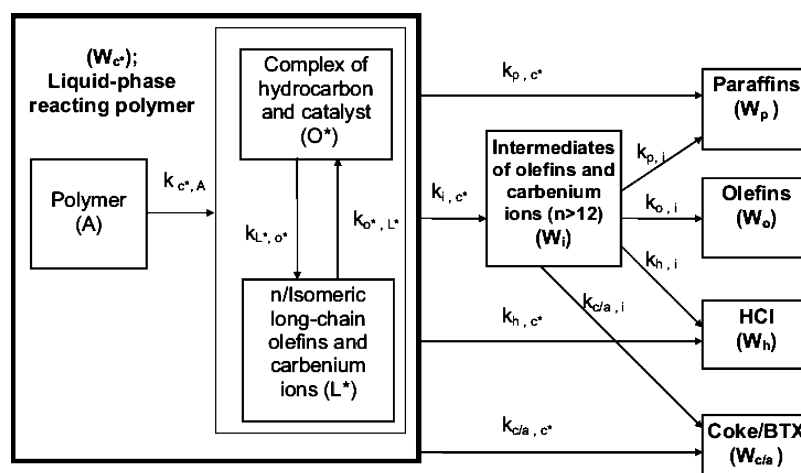


Figure 14. Reaction mechanism in the catalytic cracking of comingled plastics in a fluidized bed reactor (reprinted with permission from ref 102, copyright Elsevier).

model, it was assumed that the molten plastics after contact with the catalyst formed a polymer/catalyst complex, which underwent the reaction paths described in the mechanism. As a result of the scission reactions, different species, such as long-chain olefins and intermediate precursors for carbenium ions, were generated. According to this model, the rate of formation r_{ij} of a product i from a reactant r by means of the reaction j was given by the expression:

$$r_{ij} = k_{ij} W_r^{n_j} \eta_j$$

wherein k_{ij} represents the kinetic constant, W_r is the weight fraction of the reactant r present on the acid sites, n_j is the reaction order of the j th reaction and η_j is the activity decay of the catalyst in the j th reaction. The latter was obtained according to the following exponential decay function and was supposed to be the same for all the reaction steps (η):

$$\eta_j = \exp(-\alpha W_{\text{cok}}) = \eta$$

wherein α is a constant and W_{cok} is the content of coke over the catalyst. The different lumps of the model were the olefinic lump (W_o), the paraffinic lump (W_p), the HCl lump (W_h), the coke/BTX lump ($W_{c/a}$), the liquid phase polymer species (W_{c*}), and the intermediate of olefins and carbenium species lump (W_i).

This mechanism was applied successfully for the fitting of the experimental data obtained using as catalysts Fe-modified spent FCC catalyst, ZSM-5, and silica–alumina to obtain the respective apparent rate constants. Thus, good agreement was found with the experimental data, so it was possible to predict the performance of the catalysts by using this kinetic model. For instance, higher values of the apparent rate constants for both the paraffinic lump ($k_{p,i}$) and the coke/BTX lump ($k_{c/a,i}$) were determined for the Fe-modified spent FCC catalyst with regard to ZSM-5 and silica–alumina.

6. ZEOLITES WITH ENHANCED ACCESSIBILITY

The aforementioned catalytic results emphasize that the catalytic degradation over zeolites occurs initially at the outer surface or over the acid sites present in the pore mouths. The smaller molecules formed can subsequently enter the zeolite micropores undergoing different secondary reactions, depending on the acidity and the pore channel architecture of the

zeolite. Consequently, one initial goal in the catalytic cracking of polyolefins over zeolites was enhancing the accessibility of the zeolite acid sites. This may be accomplished by using small crystal size zeolites, wherein a high portion of external acid sites is available for the cracking. This was first proved by Songip et al.¹⁰³ in catalytic cracking at 400 °C in a fixed bed reactor of the heavy oil coming from the pyrolysis of polyethylene using rare earth metal-exchanged Y zeolites with crystal sizes of 0.1 and 1 μm , respectively. The conversion obtained with the smaller crystal size sample was higher (84.17%) than with the larger one (69.83%), whereas the selectivity to gases was superior with the former. These facts pointed out that the reaction was not only controlled by the reaction regime but also by the intraparticle diffusion.

Serrano et al.¹⁰⁴ highlighted the importance of using nanozeolites in the catalytic cracking at 400 °C of a standard mixture with makeup similar to common household wastes (46.5 wt % LDPE, 25% HDPE, and 28.5% PP) in a semibatch reaction. They observed that a nanocrystalline ZSM-5 zeolite with an average crystal size of 75 nm and a external surface area of 81 $\text{m}^2 \text{g}^{-1}$ (roughly 19% of the total BET surface area) gave rise to 84% conversion, whereas a standard HZSM-5 with a crystal size of 3 μm and an equivalent external surface area of 7 $\text{m}^2 \text{g}^{-1}$ (just 2% of the total BET surface area) gave rise to a conversion below 10%. Consequently, the much higher portion of external surface of the HZSM-5 nanozeolite, fully accessible for the polymer macromolecules, considerably improved the cracking activity. Serrano et al.¹⁰⁵ studied more deeply the influence of the crystal size with different HZSM-5 nanozeolite samples. They synthesized HZSM-5 nanozeolites with crystal sizes within 10–60 nm and having BET surface areas ranging from 78 to 242 $\text{m}^2 \text{g}^{-1}$. All these nanozeolites were extremely active and capable of promoting the catalytic degradation of both LDPE and HDPE at 340 °C, despite using a plastic/catalyst mass ratio as high as 100/1 in a stirred semibatch reaction. In addition, the activity was clearly enhanced on increasing the external surface area, and the main products were C_3 – C_5 hydrocarbons, many of them olefins.

Mastral et al.¹⁰⁶ detected in the catalytic cracking of HDPE at 500 °C in a fluidized bed reactor over nanocrystalline HZSM-5 (crystal size of 100 nm) that the selectivity was extremely dependent on the polymer/catalyst mass ratio. Thus, although a polymer/catalyst mass ratio of 0.93 led to 44.5% butene and

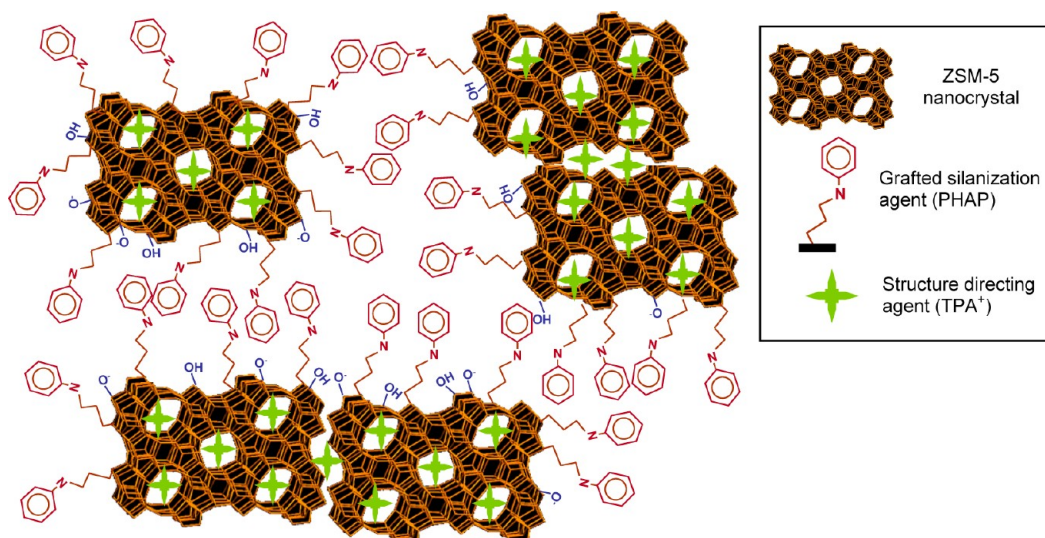


Figure 15. Anchoring of the seed silanization agent over the external surface of protozeolitic units (reprinted with permission from ref 115, copyright American Chemical Society).

9.72% propene, a slight increase in this ratio to 1.41 dropped the portion of butenes to 23.85% and raised that of propene to 18.2%. Therefore, small variations in this ratio affect meaningfully the makeup of the C_3 – C_5 primary cracking products, at least at low polymer/catalyst mass ratios.

Nanozeolite Beta (external surface of $183 \text{ m}^2 \text{ g}^{-1}$) was also studied by Marcilla et al.¹⁰⁷ in the catalytic cracking of LDPE by thermogravimetry and showed higher activity than HZSM-5 when low catalyst amounts were added, due to its remarkable external surface. Interestingly, over nanozeolite Beta, the portions of isobutane/butane and paraffins/olefins were much higher than over HZSM-5 due to its larger pore size. These results point out that the initial cracking steps occurred over the external surface and at the pore mouths, whereas secondary reactions such as hydrogen transfer took place inside the zeolite Beta micropores.

One important point to clarify is whether the small crystal size of the nanozeolites may alter the acid strength distribution of the catalyst. In this regard, Lee et al.¹⁰⁸ performed the ammonia TPD measurements of several Beta nanozeolites with different Si/Al and crystal sizes and found that the crystal size did not meaningfully vary the peak of maximum temperature of ammonia desorption, so a similar acid strength distribution is to be expected among the samples. Covarrubias et al.¹⁰⁹ investigated nanosized La-exchanged ZSM-2 (100 nm of crystal size) in the degradation of polyethylene in a semibatch reaction. ZSM-2 zeolite has a pore channel of 0.74 nm, and its framework is an intergrowth of cubic FAU and hexagonal EMT, so their results were compared with those of a micrometer Y zeolite (30 μm of crystal size). Again, the usage of a nanozeolite increased the activity, since for LaHZSM-2, the onset temperature of degradation was decreased to 391 $^\circ\text{C}$ while the corresponding one for LaHY was just 426 $^\circ\text{C}$.

One important and recent advance in the field of catalytic cracking of polyolefins has been the development and usage of hierarchical zeolites. Unlike conventional zeolites wherein only micropores and sometimes a small amount of mesopores are usually present, these catalysts are characterized by their possessing a bimodal microporous–mesoporous pore size distribution with a considerable share of mesopores. Hierarchical zeolites can be prepared by means of different

procedures, such as carbon templating,¹¹⁰ desilication,¹¹¹ or use of organosilanes.^{112–114} The most applied method for the synthesis of hierarchical zeolites subsequently used for polymer cracking has been the seed silanization procedure. In this method, a bulky seed silanization agent (e.g., phenylaminopropyltrimethoxysilane) is added to the synthesis gel of the zeolite after the precrystallization stage once the protozeolitic units have been formed, anchoring over their external surface. The anchored seed silanization agent hinders the growth of the zeolite in the zones wherein it is present (Figure 15).¹¹⁵ After calcination, the elimination of the organic seed silanization agent generates some voids that are the mesopores of the hierarchical zeolite. Figure 16 shows TEM micrographs of a hierarchical ZSM-5 zeolite prepared by a seed silanization procedure,¹¹⁶ and Figure 17 illustrates the TEM micrographs and the electron diffraction of a hierarchical ZSM-5 zeolite prepared using an amphiphile organosilane,¹¹² both of them possessing polynanocrystalline frameworks.

On the other hand, Figure 18 displays the pore size distribution obtained by means of Ar physisorption measurements at $-186 \text{ }^\circ\text{C}$ of hierarchical HZSM-5 samples prepared with different contents of a seed silanization agent (0–12%),¹¹⁷ wherein the presence of mesopores is easily appreciated. Serrano et al.¹¹⁴ tested hierarchical ZSM-5 and Beta zeolites prepared by the silanization of protozeolitic units in the catalytic cracking of PP at 360 $^\circ\text{C}$ in a stirred semibatch reaction. Hierarchical ZSM-5 gave rise to 100% conversion; the standard HZSM-5 nanozeolite showed 27.3% conversion. It must be said that this reference HZSM-5 zeolite was not a micrometer one, but was, instead, a nanozeolitic HZSM-5 sample (external surface area of $94 \text{ m}^2 \text{ g}^{-1}$) and was expected to result in a high conversion. Therefore, the hierarchical HZSM-5 improves by almost 4 times the respective values of conversion attained with the HZSM-5 nanozeolite, emphasizing how these materials are a step forward with regard to conventional nanozeolites. Lee et al.¹¹⁸ also showed higher conversions in the catalytic cracking of polyethylenes in a batch reactor over the hierarchical ZSM-5 samples than over the HZSM-5 nanozeolites (~ 200 – 500 nm of crystal size) and over large HZSM-5 crystal plates.

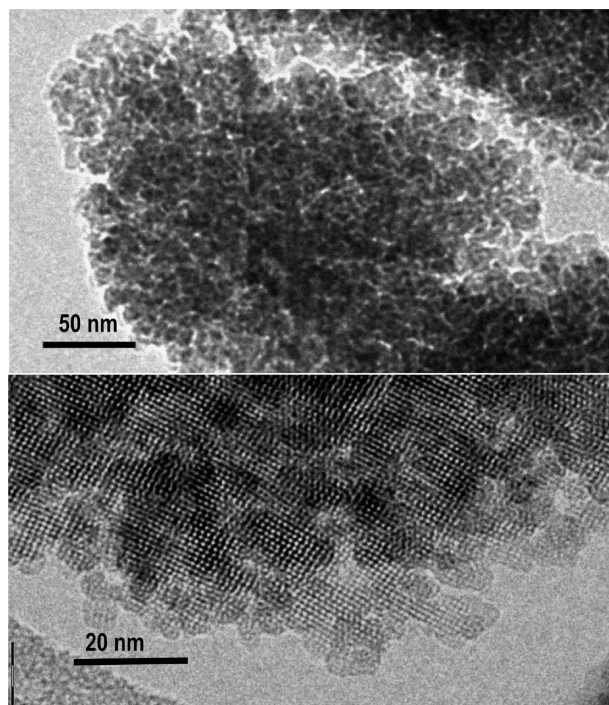


Figure 16. TEM micrographs of a hierarchical ZSM-5 zeolite prepared by a seed silanization procedure (reprinted with permission from ref 116, copyright Royal Society of Chemistry).

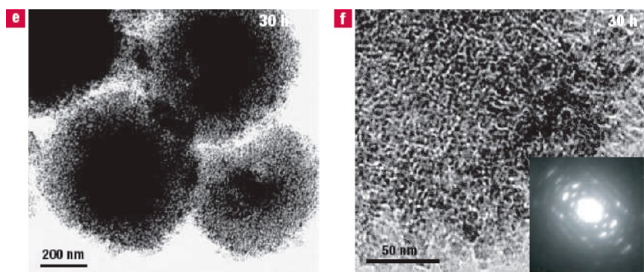


Figure 17. TEM micrographs and electron diffraction of a hierarchical ZSM-5 prepared using the amphiphile organosilane (reprinted with permission from ref 112, copyright Nature Publishing Group).

In addition, differences were also observed in the activity of the hierarchical samples, depending on the preparation procedure, since they were slightly higher for alkaline-treated samples than those prepared with a specific structure-directing agent (octadecyldimethyl 3-trimethoxysilylpropyl ammonium chloride) or from fragments of commercial HZSM-5 dissolved in NaOH 0.2 M and hexadecyltrimethylammonium bromide. Choi et al.¹¹⁹ showed that the activity in HDPE cracking in a batch reaction of the hierarchical HZSM-5 samples prepared by desilication with the optimum NaOH concentration (0.5 N) was 20 times higher than that of the parent HZSM-5 zeolite. In addition, the presence of mesopores produced enhanced yields of liquid hydrocarbons (maximum of selectivity placed at C_5 hydrocarbons) because of the shorter diffusional path of the hierarchical HZSM-5, which suppressed further secondary cracking reactions. Aguado et al.¹²⁰ prepared hierarchical mordenite zeolite by means of the seed silanization method and tested it in the catalytic cracking of LDPE in a stirred semibatch reaction. The hierarchical mordenite zeolite displayed an external surface of $57.1 \text{ m}^2 \text{ g}^{-1}$, whereas the standard mordenite had only $9 \text{ m}^2 \text{ g}^{-1}$. This difference

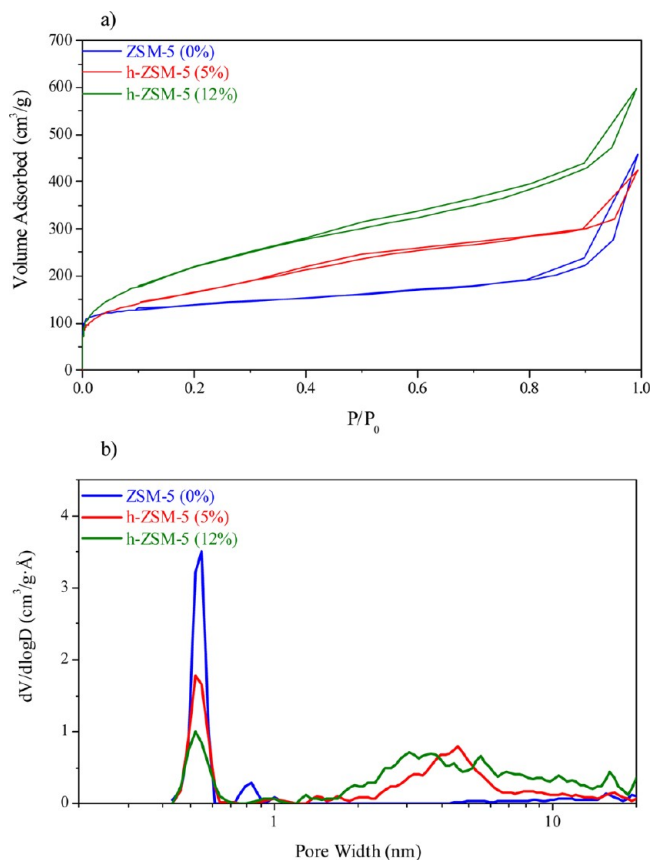


Figure 18. (a) Ar adsorption isotherms at $-186 \text{ }^\circ\text{C}$ and (b) NLDFT pore size distribution of hierarchical HZSM-5 samples prepared with different amounts of seed silanization agent (reprinted with permission from ref 117, copyright Elsevier).

produced almost double conversion over the former (57.1% vs 38.5%).

The importance of optimizing the synthesis procedure of hierarchical zeolites was highlighted by Bonilla et al.,¹²¹ who investigated the catalytic cracking of LDPE by thermogravimetry using hierarchical ferrierite samples prepared by desilication modifying the variables of the synthesis procedure. Figure 19 displays the temperatures corresponding to 50%

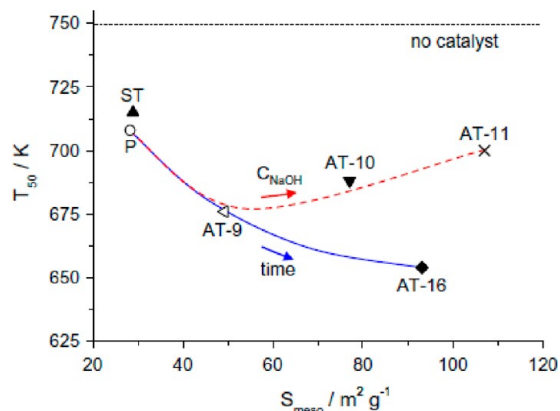


Figure 19. Correlation between the mesopore surface areas of different desilicated ferrierites and the temperatures corresponding to 50% conversion in thermogravimetric degradation of LDPE (reprinted with permission from ref 121, copyright Elsevier).

conversion of the polymer in the thermogravimetric degradation correlated with the mesopore surface area of the different desilicated ferrierite samples. These authors drew the important conclusion that the enhancement in conversion took place only when the mesopore surface area increased without a remarkable loss in micropore surface, which is equivalent to a loss of active sites. Thereby, for sample AT-11, the mesopore surface area rose to $107 \text{ m}^2 \text{ g}^{-1}$ but the micropore volume dropped to $0.08 \text{ cm}^3 \text{ g}^{-1}$ (the parent zeolite had a mesopore surface area of $20 \text{ m}^2 \text{ g}^{-1}$ and a micropore volume of $0\text{--}14 \text{ cm}^3 \text{ g}^{-1}$). In contrast, over AT-16, the mesopore surface area increased to $93 \text{ m}^2 \text{ g}^{-1}$ but the micropore volume was kept at $0.12 \text{ cm}^3 \text{ g}^{-1}$.

On the other hand, Serrano et al.,¹²² using a stirred semibatch reactor with a plastic to catalyst mass ratio of 100, concluded that the acidity of the hierarchical HZSM-5 samples exerted a deep influence on the cracking of waste polyethylene at $360 \text{ }^\circ\text{C}$. Waste plastics are more difficult to crack than pure polyolefins, since they contain impurities that may poison the catalyst, whereas its structure may have suffered changes due to environmental factors, leading to cross-linking reactions. Figure 20 depicts the activity by the aluminum atom obtained in the

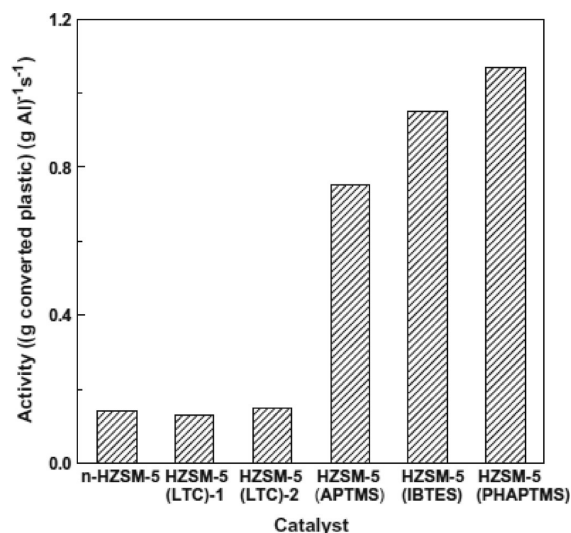


Figure 20. Activities obtained in the cracking of waste polyethylene at $380 \text{ }^\circ\text{C}$ over the different hierarchical HZSM-5 samples and standard HZSM-5 nanozeolite using a plastic/catalyst mass ratio of 100 (reprinted with permission from ref 122, copyright Elsevier).

cracking over conventional nanocrystalline HZSM-5 (*n*-HZSM-5), two hierarchical HZSM-5s prepared by a low-temperature crystallization method (HZSM-5 (LTC-1) and HZSM-5 (LTC-2)), and two hierarchical HZSM-5s prepared by the seed silanization method (HZSM-5 (APTMS) and HZSM-5 (PHAPTMS)). The hierarchical HZSM-5 samples presented external surface areas ranging from 150 to $250 \text{ m}^2 \text{ g}^{-1}$, and the conventional nanocrystalline sample showed just $78 \text{ m}^2 \text{ g}^{-1}$. The strong difference in activity observed among the hierarchical samples prepared by the silanization of protozeolitic units compared with a low temperature crystallization method was ascribed to their stronger acidity (values about $25\text{--}40 \text{ }^\circ\text{C}$ higher for the peak maximum of ammonia desorption in TPD analyses). Therefore, care must be taken in the suitable choice of the preparation method for obtaining hierarchical zeolites, since not only the mesoporous surface but also the acidity are relevant for polyolefin cracking.

7. COUPLING THERMAL AND CATALYTIC TREATMENTS

A variety of processes have been developed on the basis of the coupling of a previous thermal cracking of the waste plastics followed by a subsequent catalytic cracking. This alternative is highly recommended, since it shows several advantages.^{123,124} First, it allows decreasing the plastic viscosity, reducing thereby both mass transfer and heat transfer problems in the subsequent catalytic cracking stage. Second, the contact of the catalysts with the impurities present in the plastic wastes makeup does not occur, thus avoiding undesirable deactivation phenomena, since many of these impurities are, indeed, potential poisons for the catalysts. Finally, the recovery of the catalysts from the wastes is far easier when it is placed in a separate stage.

The presence of impurities in the raw plastic wastes is a subject of crucial importance, since they may not only deactivate the catalyst but also modify the nature of the obtained products. Thus, one of the problems associated with the polyolefin cracking of polymer mixtures coming from household wastes is the occurrence of residual amounts of PVC. PVC generates important problems, since it not only thermally decomposes at $260 \text{ }^\circ\text{C}$ ¹²⁵ into mostly HCl (which is highly corrosive) but, in addition, can also lead to the formation of unwanted chlorine-containing hydrocarbons. In this regard, Uddin et al.¹²⁶ observed in the thermal cracking of mixtures of PP/PVC and PE/PVC that 91–96% of the chlorine ended up as HCl, and the remaining chlorine was in the oils and in the final solid residue. Hence, the amount of chlorine in the oils was considerable (around 2800–12700 ppm) making this hydrocarbon mixture useless for its application as fuel. Therefore, the PVCs must be removed either by separating them properly from the plastic mixture before the cracking or by a dechlorination treatment, which would preferably take place in a previous stage before the catalytic cracking or along with the thermal cracking. The most usual way to solve this problem is by adding $\text{CaO}/\text{Ca}(\text{OH})_2$ to the thermal cracking stage.

Fujimoto et al.¹²⁷ added $\text{Ca}(\text{OH})_2$ together with the FCC catalyst to obtain liquids with less than 100 ppm of chlorine. Interestingly, Bhaskar et al.¹²⁸ described the use of a calcium carbonate composite that removed HCl and dechlorinated the obtained hydrocarbons from the cracking of a PP/PE/PS/PVC mixture at $430 \text{ }^\circ\text{C}$, yielding liquids free of chlorine. Therefore, the problem posed by the chlorine seems to be practically solved using these methods. Another and simple alternative for removing the HCl has been proposed by Lin et al.,¹²⁹ who carried out the catalytic cracking of comingled plastics ($\sim 33 \text{ wt } \% \text{ HDPE}$, $30 \text{ wt } \% \text{ LDPE}$, $34 \text{ wt } \% \text{ PP}$, and $3 \text{ wt } \% \text{ PVC}$) in a fluidized bed reactor over acid catalysts (equilibrium FCC catalyst, USY, silica–alumina, and HZSM-5). In their experimental setup, these authors installed a deionized water trap after the fluidized bed for fixing the hydrogen chloride. According to these authors, the chlorine contained in the PVC was recovered as hydrogen chloride and removed in the deionized water trap.

Another limitation to be solved for the commercial application of the hydrocarbon mixture obtained in the catalytic cracking of polyolefins as fuels is the presence of high amounts of olefins. An excessive amount of olefins in fuels is a problem, since it may cause the unwanted formation of gums inside the engines. Therefore, the content of olefins in gasolines is limited

to 18 vol %, according to EU legislation. Many of the hydrocarbon mixtures actually obtained in the catalytic cracking cannot be directly used as fuels, since they largely exceed this bound. Consequently, hydrogenation treatments of the obtained hydrocarbon mixtures are required to diminish the amount of olefins present. In this regard, Escola et al.¹⁸ devised a two-step procedure comprising first thermal cracking of the polymer in a stirred batch reactor, followed by catalytic hydroreforming of the previously obtained oils over Ni-containing mesostructured aluminosilicates (Ni/Al-SBA-15 and Ni/Al-MCM-41) and Ni-containing hierarchical zeolites (Ni/HBeta and Ni/HZSM-5) in a stirred batch reactor. This process was successful in the hydrogenation of more than 90% of the olefins originally present using Ni/HBeta, attaining 55 wt % of gasolines with a RON number of 89. In addition, this is the only two-step process currently reported wherein Ni-supported hierarchical zeolites have been used.

8. CONCLUDING REMARKS

The field of catalytic cracking of polyolefins has remained very active in recent years in terms of providing catalysts with enhanced performance. Initially, conventional zeolites and amorphous silica–alumina were used for cracking, determining the influence of the acidity and pore structure into several factors such as conversion, selectivity, and deactivation of the catalysts. Subsequently, because of the steric and diffusional hindrances posed by the bulky polymer molecules to enter the zeolite micropores, new catalysts based on ordered mesoporous materials (Al-MCM-41, Al-SBA-15); nanozeolites; and, especially, hierarchical zeolites were used to show enhanced activities with regard to conventional microporous zeolites. In this way, hierarchical zeolites can be considered a significant step forward, so new achievements are to be expected by their usage. Thereby, the future trends in the field should be addressed to further developments of hierarchical zeolites in terms of tailoring their porosity and acidity for obtaining high activities and the desired selectivity. In addition, the study of their deactivation and proper regeneration procedures is also a subject of pending study. In addition to hierarchical zeolites, other new materials with high accessibility to the active sites, such as extra-large pore zeolites,¹³⁰ pillared zeolite nano-sheets,¹³¹ or delaminated zeolites,¹³² hold promise for the catalytic cracking of polyolefins, although they have not yet been applied. On the other hand, two-step processes based on a combination of thermal treatments followed by catalytic reforming are expected to open up new possibilities for large-scale treatment of plastic wastes, since they allow the activity of the catalyst to be preserved from different deactivation phenomena.

AUTHOR INFORMATION

Corresponding Author

*Phone: +34 91 664 74 50. Fax: +34 91 488 70 68. E-mail: david.serrano@imdea.org.

Notes

The authors declare no competing financial interest.

REFERENCES

- (1) *Plastics – the Facts 2011*; Plastics Europe: Brussels, Belgium, 2011.
- (2) Aguado, J.; Serrano, D. P.; Escola, J. M. *Ind. Eng. Chem. Res.* **2008**, *47*, 7982–7992.

- (3) Al Salem, S. M.; Lettieri, P.; Baeyens, J. *Waste Manag.* **2009**, *29*, 2625–2643.
- (4) Ramírez Vargas, E.; Sandoval Arellano, Z.; Hernández Valdez, J. S.; Martínez Colunga, J. G.; Sánchez Valdés, S. *J. Appl. Polym. Sci.* **2006**, *100* (5), 3696–3706.
- (5) Dawans, F. *Rev. Inst. Fr. Pet.* **1992**, *47* (6), 937–956.
- (6) Vispute, T. P.; Zhang, H.; Sauna, A.; Xiao, R.; Huber, G. W. *Science* **2010**, *330*, 1222–1227.
- (7) Bockhorn, H.; Burckschat, M.; Dreuser, H. *J. Anal. Appl. Pyrolysis* **1985**, *8*, 427–437.
- (8) Wampler, T. P. *J. Anal. Appl. Pyrolysis* **1989**, *15*, 187–195.
- (9) Williams, P. T.; Williams, E. A. *Energy Fuels* **1999**, *13*, 188–196.
- (10) Marcilla, A.; Beltran, M. I.; Navarro, R. *J. Anal. Appl. Pyrolysis* **2009**, *86*, 14–21.
- (11) Kaminsky, W.; Predel, M.; Sadiki, A. *Polym. Degrad. Stab.* **2004**, *85*, 1045–1050.
- (12) Kaminsky, W.; Schmidt, H.; Simon, C. M. *Macromol. Symp.* **2000**, *152*, 191–199.
- (13) Corma, A. *Chem. Rev.* **1995**, *95* (3), 559–614.
- (14) Aguado, J.; Serrano, D. P.; Escola, J. M. *Ind. Eng. Chem. Res.* **2000**, *39* (5), 1177–1184.
- (15) Aguado, J.; Serrano, D. P.; Sotelo, J. L.; Van Grieken, R.; Escola, J. M. *Ind. Eng. Chem. Res.* **2001**, *40*, 5696–5704.
- (16) Aguado, J.; Serrano, D. P.; Miguel, G. S.; Escola, J. M.; Rodriguez, J. M. *J. Anal. Appl. Pyrolysis* **2007**, *78*, 153–161.
- (17) Ng, S. H.; Seoud, H.; Stanculescu, M.; Sugimoto, Y. *Energy Fuels* **1995**, *9*, 735–742.
- (18) Escola, J. M.; Aguado, J. M.; Serrano, D. P.; Garcia, A.; Peral, A.; Briones, L.; Calvo, R.; Fernández, E. *Appl. Catal., B* **2011**, *106*, 405–415.
- (19) Blazsó, M. *Feedstock Recycling and Pyrolysis of Waste Plastics*; Scheirs, J., Kaminsky, W., Eds.; John Wiley & Sons: New York, 2006; p 315.
- (20) Ivanova, S. R.; Gumerova, E. F.; Minsker, K. S.; Zaikov, G. E.; Berlin, A. A. *Prog. Polym. Sci.* **1990**, *15*, 193–215.
- (21) Adams, C. J.; Earle, M. J.; Seddon, K. R. *Green Chem.* **2000**, *21*–23.
- (22) Kaminsky, W.; Nuñez-Zorriquetta, I. J. *J. Anal. Appl. Pyrolysis* **2007**, *79* (1–2), 368–374.
- (23) Uemichi, Y.; Kashiwaya, Y.; Tsukidate, M.; Ayame, A.; Kanoh, H. *Bull. Chem. Soc. Jpn.* **1983**, *56*, 2768–2773.
- (24) Ishihara, Y.; Nanbu, H.; Saido, K.; Ikemura, T.; Takesue, T. *Bull. Chem. Soc. Jpn.* **1991**, *64*, 3585–3592.
- (25) Ishihara, Y.; Nambu, H.; Ikemura, T.; Takesue, T. *J. Appl. Polym. Sci.* **1989**, *38*, 1491–1501.
- (26) Vasile, C.; Onu, P.; Barboiu, V.; Sabliovschi, M.; Moroi, G. *Acta Polym.* **1985**, *36* (10), 543–549.
- (27) Vasile, C.; Onu, P.; Barboiu, V.; Sabliovschi, M.; Moroi, G.; Florea, M. *Acta Polym.* **1988**, *39* (6), 306–310.
- (28) Beltrame, P. L.; Carniti, P. *Polym. Degrad. Stab.* **1989**, *26* (3), 209–220.
- (29) Audisio, G.; Bertini, F.; Beltrame, P. L.; Carniti, P. *Makromol. Chem., Macromol. Symp.* **1992**, *57*, 191–209.
- (30) Uemichi, Y.; Kashiwaya, Y.; Ayame, A.; Kanoh, H. *Chem. Lett.* **1984**, 41–44.
- (31) Uemichi, Y.; Makino, Y.; Kanazuka, T. *J. Anal. Appl. Pyrolysis* **1989**, *14*, 331–344.
- (32) Nakamura, I.; Fujimoto, K. *Catal. Today* **1996**, *27*, 175–179.
- (33) Ohkita, H.; Nishiyama, R.; Tochiyama, Y.; Mizushima, T.; Kakuta, N.; Ueno, A.; Namiki, Y.; Tanifuji, S.; Katoh, H.; Sunazuka, H.; Nakayama, R.; Kuroyanagi, T. *Ind. Eng. Chem. Res.* **1993**, *32*, 3112–3116.
- (34) Mertinkat, J.; Kirsten, A.; Predel, M.; Kaminsky, W. *J. Anal. Appl. Pyrolysis* **1999**, *49*, 87–95.
- (35) Sharratt, P. N.; Lin, Y. H.; Garforth, A.; Dwyer, J. *Ind. Eng. Chem. Res.* **1997**, *36*, 5118–5124.
- (36) Elordi, G.; Olazar, M.; Lopez, G.; Amutio, M.; Artetxe, M.; Aguado, R.; Bilbao, J. *J. Anal. Appl. Pyrolysis* **2009**, *85*, 345–351.

- (37) Arandes, J. M.; Abajo, I.; Lopez-Valerio, D.; Fernandez, I.; Azkoiti, M. J.; Olazar, M.; Bilbao, J. *Ind. Eng. Chem. Res.* **1997**, *36*, 4523–4529.
- (38) Marcilla, A.; Hernandez, M. R.; Garcia, A. N. *Appl. Catal., A* **2008**, *341*, 181–191.
- (39) Arandes, J. M.; Torre, I.; Azkoiti, M. J.; Castaño, P.; Bilbao, J.; De Lasa, H. *Catal. Today* **2008**, *133–135*, 413–419.
- (40) Arandes, J. M.; Azkoiti, M. J.; Torre, I.; Olazar, M.; Castaño, P. *Chem. Eng. J.* **2007**, *132*, 17–26.
- (41) Serrano, D. P.; Aguado, J.; Escola, J. M.; Garagorri, E. *J. Anal. Appl. Pyrolysis* **2001**, *58–59*, 789–801.
- (42) Songip, A. R.; Masuda, T.; Kuwahara, H.; Hashimoto, K. *Appl. Catal., B* **1993**, *2–3*, 153–164.
- (43) Mordí, R. C.; Fields, R.; Dwyer, J. *J. Anal. Appl. Pyrolysis* **1994**, *29*, 45–55.
- (44) Aguado, J.; Serrano, D. P.; Escola, J. M.; Garagorri, E.; Fernández, J. A. *Polym. Degrad. Stab.* **2000**, *69*, 11–16.
- (45) Manos, G.; Garforth, A.; Dwyer, J. *Ind. Eng. Chem. Res.* **2000**, *39*, 1198–1202.
- (46) Bagri, R.; Williams, P. T. *J. Anal. Appl. Pyrolysis* **2002**, *63* (1), 29–41.
- (47) Hernández, M. R.; Garcia, A. N.; Marcilla, A. *J. Anal. Appl. Pyrolysis* **2007**, *78*, 272–281.
- (48) Manos, G.; Garforth, A.; Dwyer, J. *Ind. Eng. Chem. Res.* **2000**, *39*, 1203–1208.
- (49) Fernandez, G. J. T.; Fernandez, V. J.; Araujo, A. S. *Catal. Today* **2002**, *75*, 233–238.
- (50) Miskolczi, N.; Bartha, L.; Deak, G.; Jover, B.; Kallo, D. *J. Anal. Appl. Pyrolysis* **2004**, *72*, 235–242.
- (51) Mikulec, J.; Vrbova, M. *Clean Technol. Environ. Policy* **2008**, *10*, 121–130.
- (52) Hwang, E. Y.; Kim, J. R.; Choi, K.; Woo, H. C.; Park, D. W. *J. Anal. Appl. Pyrolysis* **2002**, *62*, 351–364.
- (53) Aguado, J.; Sotelo, J. L.; Serrano, D. P.; Calles, J. A.; Escola, J. M. *Energy Fuels* **1997**, *11*, 1225–1231.
- (54) Uddin, M. A.; Koizumi, K.; Murata, K.; Sakata, Y. *Polym. Degrad. Stab.* **1997**, *56*, 37–44.
- (55) Garforth, A. A.; Lin, Y. H.; Sharratt, P. N.; Dwyer, J. *Appl. Catal., A* **1998**, *169*, 331–342.
- (56) Uemichi, Y.; Nakamura, J.; Itoh, T.; Sugioka, M.; Garforth, A. A.; Dwyer, J. *Ind. Eng. Chem. Res.* **1999**, *38*, 385–390.
- (57) Aguado, J.; Serrano, D. P.; Romero, M. D.; Escola, J. M. *Chem. Commun.* **1996**, 725–726.
- (58) Soler-Illia, G. J. A. A.; Sanchez, C.; Lebeau, B.; Patarin, J. *Chem. Rev.* **2002**, *102* (11), 4093–4138.
- (59) Morales, G. Organic functionalization of mesostructured materials with sulfonic groups for catalytic processes in fine chemistry; PhD Thesis, Rey Juan Carlos University, Móstoles, Spain, 2005.
- (60) Garforth, A.; Fiddy, S.; Lin, Y. H.; Ghanbari, S. A.; Sharratt, P. N.; Dwyer, J. *Thermochim. Acta* **1997**, *294*, 65–69.
- (61) Neves, I. C.; Botelho, G.; Machado, A. V.; Rebelo, P.; Ramoa, S.; Pereira, M. F. R.; Ramanathan, A.; Pescarmona, P. *Polym. Degrad. Stab.* **2007**, *92*, 1513–1519.
- (62) Aguado, J.; Serrano, D. P.; San Miguel, G.; Escola, J. M.; Rodriguez, J. M. *J. Anal. Appl. Pyrolysis* **2007**, *78*, 153–161.
- (63) Manos, G.; Yusof, I. Y.; Papayannakos, N.; Gangas, N. H. *Ind. Eng. Chem. Res.* **2001**, *40*, 2220–2225.
- (64) Manos, G.; Yusof, Y. I.; Gangas, H. N.; Papayannakos, U. *Energy Fuels* **2002**, *16*, 485–489.
- (65) Cardona, S. C.; Corma, A. *Appl. Catal., B* **2000**, *25*, 151–162.
- (66) Cardona, S. C.; Corma, A. *Catal. Today* **2002**, *75*, 239–246.
- (67) Gobin, K.; Manos, G. *Polym. Degrad. Stab.* **2004**, *86*, 225–231.
- (68) Salmiaton, A.; Garforth, A. *Waste Manag.* **2007**, *27*, 1891–1896.
- (69) Lee, K. H.; Noh, S.; Shin, D. H.; Seo, Y. *Polym. Degrad. Stab.* **2002**, *78*, 539–544.
- (70) Lin, Y. H.; Yang, M. H. *Appl. Catal., A* **2007**, *328*, 132–139.
- (71) Achilias, D. S.; Roupakias, C.; Megalokonomos, P.; Lappas, A. A.; Antonokou, E. V. *J. Hazard. Mater.* **2007**, *149*, 536–542.
- (72) De la Puente, G.; Klocker, C.; Sedran, U. *Appl. Catal., B* **2002**, *36* (4), 279–285.
- (73) Ng, S. H. *Energy Fuels* **1995**, *9*, 216–224.
- (74) Arandes, J. M.; Torre, I.; Castaño, P.; Olazar, M.; Bilbao, J. *Energy Fuels* **2007**, *21*, 561–569.
- (75) Zhao, W.; Hasegawa, S.; Fujita, J.; Yoshii, F.; Sasaki, T.; Makuuchi, K.; Sun, J.; Nishimoto, S. *Polym. Degrad. Stab.* **1996**, *53*, 129–135.
- (76) Akpanudoh, N. S.; Gobin, K.; Manos, G. *J. Mol. Catal. A* **2005**, *235*, 67–73.
- (77) Neves, I. C.; Botelho, G.; Machado, A. V.; Rebelo, P. *Eur. Polym. J.* **2006**, *42*, 1541–1547.
- (78) Elordi, G.; Olazar, M.; Artetxe, M.; Castaño, P.; Bilbao, J. *Appl. Catal., A* **2012**, *415–416*, 89–95.
- (79) Lin, R.; White, R. L. *J. Appl. Polym. Sci.* **1995**, *58*, 1151–1159.
- (80) Coelho, A.; Costa, L.; Marques, M. M.; Fonseca, I. M.; Lemos, M. A. N. D. A.; Lemos, F. *Appl. Catal., A* **2012**, *413–414*, 183–191.
- (81) Neves, I. C.; Botelho, G.; Machado, A. V.; Rebelo, P. *Mater. Chem. Phys.* **2007**, *104*, 5–9.
- (82) Songip, A. R.; Masuda, T.; Kuwahara, H.; Hashimoto, K. *Energy Fuels* **1994**, *8*, 131–135.
- (83) Takuma, T.; Uemichi, Y.; Ayame, A. *Appl. Catal., A* **2000**, *192*, 273–280.
- (84) Renzini, M. S.; Sedran, U.; Pierella, L. B. *J. Anal. Appl. Pyrolysis* **2009**, *86*, 215–220.
- (85) Uemichi, Y.; Hattori, M.; Itoh, T.; Nakamura, J.; Sugioka, M. *Ind. Eng. Chem. Res.* **1998**, *37*, 867–872.
- (86) Ali, S.; Garforth, A.; Harris, D. H.; Lawrence, D. J.; Uemichi, Y. *Catal. Today* **2002**, *75*, 247–255.
- (87) Lin, Y. H.; Sharratt, P. N.; Garforth, A. A.; Dwyer, J. *Thermochim. Acta* **1997**, *294*, 45–50.
- (88) Lin, Y. H.; Yang, M. H. *Thermochim. Acta* **2008**, *470*, 52–59.
- (89) Elordi, G.; Olazar, M.; Lopez, G.; Castaño, P.; Bilbao, J. *Appl. Catal., B* **2011**, *102* (1–2), 224–231.
- (90) Lin, Y. H.; Yang, M. H.; Yeh, T. F.; Ger, M. D. *Polym. Degrad. Stab.* **2004**, *86*, 121–128.
- (91) Marcilla, A.; Beltran, M. I.; Navarro, R. *Appl. Catal., A* **2007**, *333*, 57–66.
- (92) Renzini, M. S.; Lericci, L.; Sedran, U.; Pierella, L. B. *J. Anal. Appl. Pyrolysis* **2011**, *92*, 450–455.
- (93) Marcilla, A.; Gómez-Siurana, A.; Valdes, F. J. *Appl. Catal., A* **2008**, *334*, 20–25.
- (94) Castaño, P.; Elordi, G.; Olazar, M.; Aguayo, A. T.; Pawelec, B.; Bilbao, J. *Appl. Catal., B* **2011**, *104*, 91–100.
- (95) Castaño, P.; Elordi, G.; Ibañez, M.; Olazar, M.; Bilbao, J. *Catal. Sci. Technol.* **2012**, *2*, 504–508.
- (96) Serrano, D. P.; Aguado, J.; Escola, J. M.; Garagorri, E. *Appl. Catal., B* **2003**, *44* (2), 95–105.
- (97) Wei, T. T.; Wu, K. J.; Lee, S. L.; Lin, Y. H. *Res. Conserv. Recycl.* **2010**, *54*, 952–961.
- (98) De la Puente, G.; Arandes, J. M.; Sedran, U. A. *Ind. Eng. Chem. Res.* **1997**, *36*, 4530–4534.
- (99) Serrano, D. P.; Aguado, J.; Escola, J. M. *Appl. Catal., B* **2000**, *25*, 181–189.
- (100) Ding, F.; Xiong, L.; Luo, C.; Zhang, H.; Chen, X. *J. Anal. Appl. Pyrolysis* **2012**, *94*, 83–90.
- (101) Yang, M. H.; Lin, Y. H. *J. Appl. Polym. Sci.* **2009**, *114*, 193–203.
- (102) Lin, Y. H.; Tseng, C. C.; Wei, T. T.; Hsu, C. T. *Catal. Today* **2011**, *174*, 37–45.
- (103) Songip, A. R.; Masuda, T.; Kuwahara, H.; Hashimoto, K. *Energy Fuels* **1994**, *8*, 136–140.
- (104) Serrano, D. P.; Aguado, J.; Escola, J. M. *Ind. Eng. Chem. Res.* **2000**, *39*, 1177–1184.
- (105) Serrano, D. P.; Aguado, J.; Escola, J. M.; Rodriguez, J. M. *J. Anal. Appl. Pyrolysis* **2005**, *74*, 353–360.
- (106) Mastral, J. F.; Berruoco, M.; Gea, M.; Ceamanos, J. *Polym. Degrad. Stab.* **2006**, *91*, 3330–3338.
- (107) Marcilla, A.; Gomez Siurana, A.; Valdes, F. J. *Appl. Catal. A* **2007**, *79*, 433–442.

- (108) Lee, Y. J.; Kim, H.; Kim, S. H.; Hong, S. B.; Seo, G. *Appl. Catal., B* **2008**, *83*, 160–167.
- (109) Covarrubias, C.; Gracia, F.; Palza, H. *Appl. Catal., A* **2010**, *384*, 186–191.
- (110) Jacobsen, C. J. H.; Madsen, C.; Houzvizka, J.; Schmidt, I.; Carlsson, A. J. *Am. Chem. Soc.* **2000**, *122*, 7116–7117.
- (111) Groen, J. C.; Jansen, J. C.; Moulijn, J. A.; Perez Ramirez, J. J. *Phys. Chem. B* **2004**, *108*, 13062–13065.
- (112) Choi, M.; Cho, H. S.; Srivastava, R.; Venkatesan, C.; Choi, D. H.; Ryoo, R. *Nat. Mater.* **2006**, *5*, 718–722.
- (113) Wang, H.; Pinnavaia, T. J. *Angew. Chem., Int. Ed.* **2006**, *45*, 7603–7606.
- (114) Serrano, D. P.; Aguado, J.; Escola, J. M.; Rodriguez, J. M.; Peral, A. *Chem. Mater.* **2006**, *18*, 2462–2464.
- (115) Serrano, D. P.; Aguado, J.; Morales, G.; Rodriguez, J. M.; Peral, A.; Thommes, M.; Epping, J. D.; Chmelka, B. F. *Chem. Mater.* **2009**, *21*, 641–654.
- (116) Serrano, D. P.; Aguado, J. M.; Escola, J. M.; Rodriguez, J. M.; Peral, A. *J. Mater. Chem.* **2008**, *18*, 4210–4218.
- (117) Serrano, D. P.; Garcia, R. A.; Vicente, G.; Linares, M.; Prochazkova, D.; Cejka, J. *J. Catal.* **2011**, *279*, 366–380.
- (118) Lee, J. Y.; Park, S. M.; Saha, S. K.; Cho, S. J.; Seo, G. *Appl. Catal., B* **2011**, *108* (1–2), 61–71.
- (119) Choi, D. H.; Park, J. W.; Kim, J. H.; Sugi, Y.; Seo, G. *Polym. Degrad. Stab.* **2006**, *91*, 2860–2866.
- (120) Aguado, J.; Serrano, D. P.; Escola, J. M.; Peral, A. *J. Anal. Appl. Pyrolysis* **2009**, *85*, 352–358.
- (121) Bonilla, A.; Baudouin, D.; Perez Ramirez, J. J. *Catal.* **2009**, *265*, 170–180.
- (122) Serrano, D. P.; Aguado, J.; Escola, J. M.; Rodriguez, J. M.; Peral, A. *J. Catal.* **2010**, *276*, 152–160.
- (123) Hirota, T. *Makromol. Chem. Macromol. Symp.* **1992**, *57*, 161–173.
- (124) Aguado, J.; Serrano, D. P.; San Miguel, G.; Castro, M. C.; Madrid, S. J. *Anal. Appl. Pyrolysis* **2007**, *79* (1–2), 415–423.
- (125) Bockhorn, H.; Hornung, A.; Hornung, U.; Jakobstroer, P.; Kraus, M. J. *Anal. Appl. Pyrolysis* **1999**, *49*, 97–106.
- (126) Uddin, M. A.; Sakata, Y.; Shiraga, Y.; Muto, A.; Murata, K. *Ind. Eng. Chem. Res.* **1999**, *38*, 1406–1410.
- (127) Fujimoto, K.; Haga, H.; Tani, H.; Yamawaki, T. *Proceedings of the 4th International Symposium on Feedstock Recycling of Plastics & Other Polymeric Materials (ISFR 2007)*, Jeju, Korea, 2007, p 123.
- (128) Bhaskar, T.; Uddin, M. A.; Kaneko, J.; Kusaba, T.; Matsui, T.; Muto, A.; Sakata, Y.; Murata, K. *Energy Fuels* **2003**, *17*, 75–80.
- (129) Lin, Y. H.; Yang, M. H.; Wei, T. T.; Hsu, C. T.; Wu, K. J.; Lee, S. L. *J. Anal. Appl. Pyrolysis* **2010**, *87*, 154–162.
- (130) Corma, A.; Diaz Cabañas, M. J.; Jordá, J. L.; Martínez, C.; Moliner, M. *Nature* **2006**, *443*, 842–845.
- (131) Na, K.; Choi, M.; Park, W.; Sakamoto, Y.; Terasaki, O.; Ryoo, R. *J. Am. Chem. Soc.* **2010**, *132* (12), 4169–4177.
- (132) Corma, A.; Fornes, V.; Pergher, S. B.; Maesen, Th. L. M.; Buglass, J. G. *Nature* **1998**, *396*, 353–356.